
# PERFORMANCE ANALYSIS OF A mmWAVE-NOMA NETWORK FOR REAL-TIME IoT APPLICATIONS

by

**FARIHA TABASSUM**
*(B.Sc. Engg., MIST)*

A THESIS SUBMITTED IN PARTIAL FULFILMENT
OF THE REQUIREMENT FOR THE DEGREE OF

**MASTER OF SCIENCE**

IN

ELECTRICAL ELECTRONIC AND COMMUNICATION ENGINEERING

DEPARTMENT OF
ELECTRICAL ELECTRONIC AND COMMUNICATION ENGINEERING
MILITARY INSTITUTE OF SCIENCE AND TECHNOLOGY
MIRPUR CANTONMENT, DHAKA-1216
SEPTEMBER 2020

# APPROVAL

The thesis titled **"Performance Analysis of a mmWave-NOMA Network for Real-Time IoT Applications"** submitted by Fariha Tabassum, Student ID : 1015160002(P), Session: 2015-2016, has been accepted as satisfactory in partial fulfillment of the requirements for the degree of Master of Science in Electrical, Electronic and Communication Engineering on 20 September 2020.

## BOARD OF EXAMINERS

| | |
|---|---|
| M Shamim Kaiser, PhD<br>Professor<br>IIT, JU, Dhaka - 1342 | Chairman<br>(Supervisor) |
| Brigadier General A K M Nazrul Islam, PhD<br>Senior Instructor & Head<br>Department of EECE, MIST, Dhaka - 1216 | Co-supervisor<br>Member<br>(Ex-officio) |
| Colonel Md Golam Mostafa (LPR), PhD<br>Professor<br>Department of EECE, MIST, Dhaka - 1216 | Member<br>(Internal) |
| Dr. Satya Prasad Majumder<br>Professor<br>Department of EEE, BUET, Dhaka - 1205 | Member<br>(External) |

# DEDICATION

*To my parents and family*

# DECLARATION

I hereby declare that this thesis is my original work and it has been written by me in its entirety. I have duly acknowledged all the sources of information which have been used in the thesis. The thesis (fully or partially) has not been submitted for any degree or diploma in any university or institute previously.

Fariha Tabassum
ID: 1015160002

# ACKNOWLEDGEMENTS

Firstly, I am grateful to Almighty Allah for my good health and well-being that were necessary to complete the thesis. I would like to express my sincere gratitude to my supervisor, Dr. M. Shamim Kaiser, Professor, Institute of Information Technology, Jahangirnagar University, for his invaluable contribution to my research and personal development. His continuous support, great encouragement, patience and immense knowledge made it possible to accomplish this thesis work. His affectionate guidance helped me in all the time of study and writing of this thesis. I could not have imagined having a better supervisor and mentor.

I would like to thank my co-supervisor Brig Gen Dr A K M Nazrul Islam for his insightful directions and constructive comments towards the thesis. His advices were always helpful and improved the quality of this work immensely. Without his monitoring, this work could not own the standard where it is now.

There are several people who have been important in completion of this dissertation, both academically and personally. This work and the time that I have spent in research work, would have been poorer without them. My sincere thanks go to the Department of electrical electronic and communication engineering, Military Institute of Science and Technology for providing their enormous support during the thesis work.

Last but not the least, I would like to thank my family and my in-laws for their unceasing encouragement, appreciable patience, support and attention. My sincere thanks and gratitude go to my husband for his constant support, endless love, patience and sacrifices during my thesis time period. Thanks for always believing in me, encouraging me and helping me overcome all the difficulties in my life.

# ABSTRACT

The fifth generation (5G) cellular network is expected to meet the demand for ultra-high data rate, low latency and bulk connectivity due to the massive deployment of internet of things (IoT) sensors and devices. The existing orthogonal multiple access (OMA) techniques fall short to achieve these demands. Thus, 5G comes with some unique exciting features to entertain this gigantic connectivity and low latency network. Non-orthogonal multiple access (NOMA) has been acknowledged as a promising feature to significantly enhance the network capacity. Moreover, 5G offers an extension to the current bandwidth (sub 6 GHz) by enabling millimeter wave (mmWave) communication. This unutilized mmWave high frequency bands (30-300 GHz) can carry huge data with an increased bandwidth which paves the way for massive multiple input multiple output (massive MIMO) which facilitates high spectral efficiency (SE) and lowers path loss of mmWave transmission. But this gives rise to the power-hungry radio frequency chain which, in turn, increases the energy consumption with an increased receiver complexity. An energy efficient beamforming technique is, therefore, vital for an efficient network with high SE. Interference mitigation is another prime concern for better performance in 5G network. The existing interference mitigation techniques for OMA are not fully compatible for NOMA network. Thus, a proper interference mitigation technique is essential to increase the sum rate of the network.

In this thesis, a mmWave-MIMO-NOMA system model is presented which provides better the sum rate than some existing counterpart. To deal with the energy consumption, an energy efficient massive MIMO network with a fuzzy logic switching based hybrid beamforming (FeE-HBS) is presented. To mitigate the intra-cell interference created by the non-orthogonal users of NOMA, successive interference cancellation (SIC) is applied in the NOMA receivers. A modified fractional frequency reuse (FFR) technique is proposed to avoid the inter cell interference (ICI) which provides lesser bandwidth splitting than the conventional techniques. This lower splitting enables huge nodes to accumulate per sectors of a cell with reduced interference. Thus it improves the network performance while ensuring minimum ICI.

This work develops a mmWave-MIMO-NOMA network with better system capac-

ity. The FeE-HBS system enables lower number of the power-hungry phase shifters when the requirement is less. This makes the system more energy efficient with almost the same SE as the conventional digital beamforming design. Lastly, the interference mitigation is achieved by implementing SIC and a novel sectored FFR. This novel FFR technique ensures lower interference at a better system throughput than other existing techniques.

# TABLE OF CONTENTS

# LIST OF FIGURES

# LIST OF TABLES

# LIST OF ABBREVIATIONS

| | |
|---|---|
| **3GPP** | The Third Generation Partnership Project |
| **ABS** | Analog Beamforming Structure |
| **ADC** | Analog-to-Digital Converter |
| **AMPS** | Advanced Mobile Phone Service |
| **AoA** | Angle of Arrival |
| **AoD** | Angle of Departure |
| **AWGN** | Additive White Gaussian Noise |
| **BER** | Bit Error Rate |
| **BS** | Base Station |
| **BW** | Bandwidth |
| **CE** | Cell Edge |
| **CI** | Cell Interior |
| **CIR** | Channel Impulse Response |
| **CSI** | Channel State Information |
| **DAC** | Digital-to-Analog Converter |
| **DBS** | Digital Beamforming Structure |
| **EE** | Energy Efficiency |
| **FC-HBS** | Fully Connected Hybrid Beamforming Structure |
| **FeE-HBS** | Fuzzy Based Energy Efficient Hybrid Beamforming Structure |
| **FFR** | Fractional Frequency Reuse |
| **FLC** | Fuzzy Logic Controller |
| **FPA** | Fractional Power Allocation |
| **FRF** | Frequency Reuse Factor |
| **GPS** | Global Positioning System |
| **HBS** | Hybrid Beamforming Structure |
| **ICI** | Inter Cell Interference |
| **IM** | Interference Management |
| **LDC** | Low Density Spreading |
| **LoS** | Line-of-Sight |
| **LTE** | Long Term Evolution |
| **LTE-A** | Long Term Evaluation Advanced |
| **MA** | Multiple Access |
| **MFFR** | Modified Sectored Fractional Frequency Reuse |

| | |
|---|---|
| **MIMO** | Multiple Input Multiple Output |
| **mmWave** | Millimeter Wave |
| **MRC** | Maximal Ratio Combining |
| **MUD** | Multi User Detection |
| **MUSA** | Multi-User Shared Access |
| **NLOS** | Non-Line-of-Sight |
| **NOMA** | Non-Orthogonal Multiple Access |
| **nRT** | Non-Real Time |
| **OFDM** | Orthogonal Frequency Division Multiple Access |
| **OMA** | Orthogonal Multiple Access |
| **PA** | Power Allocation |
| **PAPR** | Peak-to-Average-Power Ratio |
| **PDMA** | Pattern Division Multiple Access |
| **PD-NOMA** | Power Domain Non-Orthogonal Multiple Access |
| **PS** | Phase Shifter |
| **QAM** | Quadrature Amplitude Modulation |
| **QoE** | Quality of Experience |
| **QoS** | Quality of Service |
| **QPSK** | Quaternary Phase Shift Keying |
| **RAN** | Radio Access Network |
| **RB** | Resource Block |
| **RF** | Radio Frequency |
| **RT** | Real Time |
| **SC** | Superposition Coding |
| **SC-HBS** | Sub-Connected Hybrid Beamforming Structure |
| **SCMA** | Sparse Code Multiple Access |
| **SDMA** | Space Division Multiple Access |
| **SE** | Spectral Efficiency |
| **SFR** | Soft Frequency Reuse |
| **SIC** | Successive Interference Cancellation |
| **SINR** | Signal-to-Interference-And-Noise Ratio |
| **SNIR** | Signal-to-Noise-Plus-Interference-Ratio |
| **SNR** | Signal-to-Noise Ratio |
| **TDMA** | Time Division Multiple Access |
| **UE** | User Equipment |
| **WiFi** | Wireless Fidelity |
| **WiMAX** | Worldwide Interoperability for Microwave Access |
| **xG** | x=1/2/3/4/5 Generation Mobile System |

# LIST OF NOTATIONS

| | |
|---|---|
| $\mathbf{a}_r(\phi_l^r)$ | array response vectors of BS |
| $\mathbf{a}_t^H(\phi_l^t))$ | array response vectors of user |
| $\alpha_{FPA}$ | decaying factor |
| $\alpha_l$ | complex gain for $l^{th}$ path |
| $\beta$ | power coefficient |
| $\mathbf{F}$ | hybrid beamforming matrix |
| $\mathbf{F}_{AB}$ | analog beamforming matrix |
| $\mathbf{F}_{DB}$ | digital beamforming matrix |
| $g_{\varphi_i}(u_{\varphi_i}(l))$ | equivalent channel gain after MRC |
| $\mathbf{H}$ | channel matrix |
| $h_k$ | channel gain of $k$-th user |
| $h_{\varphi_i}(u_{\varphi_i}(l))$ | the channel gain of user $u_{\varphi_i}(l)$ |
| $\|\|h_{\varphi_i}(u_{\varphi_i}(l))\|\|^2$ | equivalent channel gain after MRC |
| $k$ | number of users |
| $n_k$ | Additive White Gaussian Noise |
| $N_r$ | number of receive antennas |
| $N_t$ | number of transmit antennas |
| $N_t^{RF}$ | number of RF chains |
| $P_k$ | transmit power of user $k$ |
| $R_K$ | data rate of $K^{th}$ user |
| $R_{\varphi_i,U_{\varphi_i}}(u_{\varphi_i}(l)))$ | sum rate of user $u_{\varphi_i}(l)$ at user set $U_{\varphi_i}$ |
| $U_{\varphi_i}$ | set of users at $\varphi_i$ |
| $\mathbf{W}$ | hybrid combiner |
| $\mathbf{W}_{AB}$ | analog RF combiner |
| $\mathbf{W}_{DB}$ | digital combiner |
| $w_{\varphi_i}(u_{\varphi_i}(l))$ | the noise and ICI of user $u_{\varphi_i}(l)$ |
| $x_k$ | transmitted signal of user $k$ |
| $y_{\varphi_i}(u_{\varphi_i}(l))$ | received signal of user $u_{\varphi_i}(l)$ |
| $z_{\varphi_i}(u_{\varphi_i}(l))$ | equivalent noise and ICI gain after MRC |
| $\sigma_n^2$ | variance |
| $\gamma$ | a normalization factor |
| $\varphi_i$ | $i^{th}$ set of sub-bands |
| $\phi_l^r$ | $l^{th}$ paths angle of departure (AOD) |
| $\phi_l^t$ | $l^{th}$ paths angle of arrival (AOA) |

# CHAPTER 1

# INTRODUCTION

## 1.1 Introduction

The urge for obtaining higher data rates, accumulating more users and utilizing the available resources in the most efficient way, has driven us from one generation to another. Cellular technology is currently fighting with a new challenge, to ensure a hyper-connected network where real time communication with massive internet of things (IoT) devices is possible, which is pushing the current network to move toward the next generation. It all began with the bulk sized analog mobile phones in 1st generation cellular communication (1G) which allowed the voice calls only. The digital 2nd generation (2G) era was introduced with text message facility along with voice communication. The third generation (3G) empowered all the smartphone technologies (web browsing, video streaming, downloading and uploading contents etc.) and enhanced the capacity extensively. But due to the incorporation of huge data enabled by 3G, it was necessary to move towards the next generation, i.e. the 4th generation (4G) wireless network which is basically an extension of 3G with enlarged bandwidth and added features. 4G brought a revolutionary change in wireless communication by increasing the transmission rates 10 times than the speed of 3G technologies [2]. Despite serving huge devices with large spectral efficiency (SE), 4G is not capable enough to entertain the bulk connectivity requirement caused by the enormous development of IoT devices which leads us to move towards the next generation i.e. the 5th generation cellular network (5G). To get rid of the connectivity restriction imposed by 4G-LTE [1], non-orthogonal multiple access (NOMA) can become a promising approach offered by 5G. NOMA can serve multiple users with the same resources (frequency, time etc.) which enables the accumulation of huge IoT nodes.

Millimeter wave (mmWave) communication is another key feature of 5G which is capable of serving a huge range of devices by providing the large unutilized band-

width spectrum for mobile communication. This shorter wavelength spectrum employ a large antenna element at the transmitters and receivers [3]. This paves the way for another 5G feature i.e. massive multiple-input multiple-output (MIMO) [4]. But the high frequency mmWave spectrum can face severe path loss for its shorter wavelength. To reduce the path loss, these antenna elements transmit directional beams by applying beamforming. This beamforming can be done using the phase shifters in analog domain or in the digital domain using a radio frequency chain per antenna. These aforementioned methods are energy consuming and complex in structure. A combination of these two architectures leads to hybrid beamforming which assures better SE at less complex structure.

Another challenge arises from accumulating massive devices in the 5G wireless network which is the mitigation of the interference. It has become a major concern in 5G networks as multiple users are to be served by the same resources. Several interference management techniques can be applied to keep the network interference free while ensuring high capacity. Frequency reuse is proved to be a better option for mitigating the interference.

## 1.2 Related Works

Over the past few years NOMA has been selected as a promising multi-access strategy for 5G systems and has since been extensively tested in both single-cell and multi-cellular networks [5–10]. NOMA was addressed in two domains namely NOMA [6,11–16] power domain and NOMA [17–20] code domain [17–20]. The power domain NOMA has attracted numerous attractions and widely researched [6, 13, 16, 21]. The transmitter-side superposition code (SC) and the receiver-side successive interference cancellation (SIC) are addressed briefly at [9, 22, 23]. It has been proven that NOMA generates much higher performance than OMA network. In [9], Higuchi et al. showed that, in the case of the asymmetric channel, NOMA may generate as much as double the amount of throughput as OMA for a fixed throughput value of the weak consumer. Authors further demonstrated that the bandwidth in OMA is limited by around 2 Mb/s for a maximum 6 b/s/Hz throughput.

It has been verified that applying NOMA in mmWave communications (mmWave-NOMA) can significantly enhance the capacity compared with mmWave orthogonal multiple access (mmWave-OMA) [24–26]. In [27], Naqvi et al. compared the performance of mmWave NOMA and ultra-high frequency (UHF) NOMA. Authors have demonstrated that for a transmit power of 24 dBm and 40-user cell, sum capacity

is almost 38% greater in mmWave-NOMA than UHF-NOMA. However, the rate of decrease in sum rate with increase in cell radius is higher in mmWave NOMA than UHF-NOMA. They showed that for a shift of cell radius from 1km to 1.5 km, the sum-rate is reduced by almost 78% in mmWave-NOMA network. mmWave transmission is also studied in OMA technique [28]. But it is not feasible to incorporate mmWave transmission with OMA schemes [28] due to the directional beam of mmWave transmission and lower SE of OMA techniques than NOMA.

Beamforming turns out to be an indispensable tool for mmWave-MIMO transmission to reduce its path loss with its directional beams. Several beamforming techniques have been studied to enhance the SE [29–31]. The features of beamforming in mmWave-NOMA transmission has been studied in [25,32]. The SE is enhanced by enabling multi-beam reconfigurable antenna in [33]. Lens-based antenna is proposed in multi-beam MIMO systems which can lower the path loss and shadowing in mmWave high frequency spectrum [3, 34].

A proper choice of beamforming can reduce energy consumption without reducing the SE of the MIMO network. Many prior studies have been performed on mmWave-NOMA with analog beamforming structure (ABS). The mmWave-NOMA can outperform mmWave-OMA in terms of sum rates, respecting to a targeted data rate of the strong user in [35] using ABS. An energy-efficient analog beamforming approach is studied in [35, 36] which produces very low SE. The fully digital beamforming is proved to have better SE [37]. But its higher cost, energy consuming characteristics of radio frequency (RF) chains (nearly 250 mW per RF chain [38]) do not make it feasible to implement in large antenna array [39]. Therefore, the digital precoding is highly energy inefficient e.g., 16 W is required by a mmWave massive MIMO system with 64 antennas [40]. So hybrid analog/digital beamforming was proposed in [24,39,41,42] which shows that the hybrid beamforming structure (HBS) can achieve higher SE at reduced energy consumption in multi-user system. In [43], the authors considered the problems of user pairing, hybrid beamforming and power allocation separately in an mmWave-NOMA system. In [28], a multi-beam NOMA framework for hybrid mmWave systems was proposed, where a beam splitting technique was introduced to generate multiple analog beams to facilitate the NOMA transmission. In [44], a mmWave-NOMA with HBS structures is studied. A user grouping algorithm and power allocation was proposed which enhances the sum-rate and energy efficiency of the network compared to OMA network. In [45–47], a power allocation strategy is presented where the mmWave-NOMA network is incorporated with hybrid beamforming MIMO systems to enhance energy efficiency. Hybrid beamforming is

also studied in mmWave NOMA network in [25, 28, 32, 43]. A further energy efficient NOMA is proposed in this work with an intention of lowering the energy consumption more than the existing works.

To protect the system from ICI, interference mitigation has always been a major concern for both OMA and NOMA network. Especially, for OMA networks, ICI is the major source of interference. Several frequency reuse techniques have been studied in [48–56] for both OMA and NOMA networks. Fractional frequency reuse (FFR) [57] and soft frequency reuse (SFR) [50] were explored to avoid the interference of orthogonal frequency division multiple access (OFDMA) network. A dynamic FFR was initiated in [58] for OFDMA network based on the limitation of static FFR in real communication environment. However, this dynamic FFR mentioned in [58] can not be adapted for NOMA network because of the presence of non-orthogonal users. An adaptive resource allocation algorithm was proposed in [59] for NOMA network only which focused on edge users' performance. An FFR-based user clustering is proposed for the NOMA network in [56] which also propose a dynamic resource allocation. However, this work also depicts the NOMA performance for an ideal communication scenario. There is no prior work for NOMA with sectored FFR. Therefore, an appropriate frequency reuse technique for a real communication environment is also proposed in the thesis.

## 1.3 Problem Statement

The assemblage of huge IoT devices while ensuring real time communication is the demand of time. Researchers have been exploring newer technologies to increase the capacity at minimum latency possible. In this thesis, we have also opted for a more efficient network with higher spectral efficiency and improved data rate.

Again, focusing only on the capacity enhancement can make the system power hungry. It has been approximated that, the radio frequency chains in MIMO is capable of consuming up to 70% of the total transceiver energy. Digital beamforming can result into the maximum throughput among all the different beamformers. But it consumes huge amount of energy which makes it impractical to implement in practical scenario. Thus, it is necessary to make a trade-off between the energy efficiency and spectral efficiency. Based on this problem statement, designing a more energy efficient network by implementing a smart beamforming is focused in the work.

Interference has always been experienced as an opponent in the way of enjoying an advanced network with more IoT nodes communicating with high data rates. So

the mitigation of interference in 5G multi-cellular network becomes the next problem statement in this thesis. Moreover, sometimes mitigating interference leads to compromise with bandwidth efficiency. So, a interference mitigation technique is needed to be designed which minimizes the interference while maintaining moderate bandwidth efficiency. Lastly, real communication environment is lot more different than the ideal scenario. The users can not just be categorized basing on one parameter. They have several requirements while connecting to the network. So, users scheduling algorithm can be implemented taking into account several connectivity criteria of users which will benefit the real communication scenario.

## 1.4 Research Objectives

The research presented in this thesis tends to develop a interference free network which is capable of accumulating bulk amount of devices with lower latency with minimum energy consumption.
With this aim, the objectives of this work are outlined as follows.

i. To design a conceptual NOMA-mmWave system model for real time IoT applications. The line-of-sight (LOS) and non-line-of-sight (NLOS) users will be considered the strong and weak users respectively.

ii. To improve the Energy Efficiency under users' QoS requirements by formulating a resource allocation algorithm and hybrid beamforming under perfect and imperfect channel state information (CSI).

iii. To achieve lower latency for the mmWave-NOMA transmission compared to the equivalent system with existing OMA technologies.

iv. To compare the performance of the proposed system with the existing real time IoT applicants.

## 1.5 Research Outline

In this thesis paper, we have divided the whole paper into five chapters to make the explanation of the concepts in a convenient manner. The initial chapter provides brief discussion of the topic related to our thesis work, the motivation behind the study and the objectives we tried to achieve.

In **CHAPTER 2** the background of the proposed multiple access technique NOMA along with the other existing technologies are explained. Several classification of NOMA is also described for single cell and multi-cell wireless networks.

**CHAPTER 3** provides a brief discussion of the most popular technologies offered by 5G. mmWave transmission, MIMO, beamforming and their incorporation is well analysed. Several beamforming techniques are explained and the reason of the proposed beamforming is justified. Also, a new fuzzy based beamforming is presented in this chapter.

In **CHAPTER 4**, the ICI mitigation techniques are analyzed. It has been found that the frequency reuse techniques are a great way to overcome the ICI. The frequency reuse techniques are classified and a novel frequency reuse technique is presented.

**CHAPTER 5** compiles the proposed fuzzy based hybrid beamforming system model mention in chapter 3 and the interference mitigation technique in chapter 4. Also a user scheduling and power allocation is proposed in real communication environment basing on users' traffic class and data rate requirement.

**CHAPTER 6** presents the result we have found from this thesis. The performance of the proposed technique is validated in terms of some important parameters i.e. spectral efficiency, signal to noise and interference ratio, sum-rate, energy efficiency etc. which are some prime variables for the better performance of 5G. The proposed network is found to be of a higher capacity and lower ICI network.

**CHAPTER 7** presents the conclusion of the thesis with a summary of the original contributions and future work. Appendix and references are duly attached to the attached in the later portion of this thesis.

# CHAPTER 2

# MULTIPLE ACCESS IN LTE AND BEYOND

## 2.1 Introduction

Multiple access techniques permit multiple users to share a finite amount of resources in the most efficacious way. The radio access network (RAN) uses a suitable multiple access technique to connect the user equipment (UE) to the core network [21]. Thus, the choice of a proper multiple access technique becomes one of the most salient parameters to enhance the overall system capacity. In fact, the cellular system of each generation is moved along with the advances of these techniques. The advanced mobile phone service (AMPS) i.e. 1G started with frequency division multiple access (FDMA) which allowed only one user per channel of typically 25kHz. 2G, also known as global system for mobile communication (GSM), embraced the time division multiple access (TDMA) [15]. It served eight users by one channel of 200kHz. Code division multiple access (CDMA) was introduced in 2G but eventually adopted by 3G [60]. The 3G solution, called universal mobile telecommunication system (UMTS) by the 3rd Generation Partnership Project (3GPP) provided wider bandwidth (5 MHz) than 2G [61]. 4G offered a major breakthrough by selecting orthogonal frequency division multiple access (OFDMA) as its MA technique which enabled more wider bandwidth (10 20 MHz) [61]. The current 4G Long Term Evolution (LTE) is gradually evolving towards LTE-Advanced (LTE-A) by incorporating more exciting features in it. Nonetheless, these features fall short to move towards 5G due to the connectivity restrictions offered by 4G. Non orthogonal multiple access (NOMA), has been recognized as a promising alternative solution to entertain these gigantic connectivity requirement for the 5G wireless network.

## 2.2 Orthogonal Multiple Access

Orthogonal multiple access (OMA) has been serving the wireless communication system over the past decades with differently adopted methodology. FDMA, TDMA, CDMA, OFDMA etc are the most common approaches of it. OMA allows a perfect receiver to distinguish unwanted signals from the desired signal completely without any interference. FDMA operates by using unique frequency channels by individual users at the same time slot while in TDMA, several users share the same frequency band on a time-sharing basis. CDMA designate distinctive sequence to each user and the users transmits their signals with distinct codes but with same time/frequency resources [16].

Space division multiple access (SDMA) is another widely discussed MA technique nowadays. In SDMA, several users are served simultaneously in the same channel by enabling the superposition of the beam, resulting in an efficient use of available bandwidth. It enables the frequency reuse in a particular cell, thus increasing the capacity of the overall system.

However, despite the dissimilarities in sharing the resources (time, frequency, code etc.), all the approaches have been evolved from the same concept of generating orthogonal signals to distinguish different users at the receivers with minimum interference. In particular, OFDMA is being widely used by LTE for its higher capacity and lower interference among users. OFDMA accelerates multi-user communication by assigning non–overlapping orthogonal sub-bands to different users which, in turn, increases the number of sub-carriers extensively with lower interference. A given frequency band is divided into multiple orthogonal sub-carriers with bandwidth of 15 kHz and each sub-carrier can be allocated to at most one user only. The receivers differentiate the signal by identifying its specific frequency bands. So apparently, this OMA based system do not face interference among users because of the use of non-overlapping resources and thus, low-complexity receivers can be assigned to detect the signal of the desired user. The current LTE, also called as LTE-A still uses OFDMA with the sub-carrier range of 1.25 MHz and 20 MHz [62]. Enabling of advanced technology in LTE-A such as multiple-input multiple-output (MIMO), frequency reuse etc can result into a peak data rate of Gbps.

## 2.3 Non-orthogonal Multiple Access

Non-orthogonal multiple access (NOMA) has achieved considerable amount of interest worldwide in the wireless communication research direction due to its ability to incorporate huge number of wireless devices over the same network which is a prime requirement of 5G. Serving larger number of UE than the number of available resources makes NOMA the most appealing MA technology for the next generation. It allows several users to share the same time and frequency resources in the same instant via power-domain or code-domain multiplexing. The most popular methodology in downlink transmission is multiuser superposition transmission (MUST) in power domain [16], and it was included in 3GPP release 13. The interference can be mitigated by many interference cancellation schemes, the most popular is the successful interference cancellation (SIC) technique, which, in turn, increases its receivers complexity slightly. But overall, NOMA boosts up the user throughput, enhances spectral efficiency, relaxes channel state information (CSI) and lessens latency extensively [6, 63] compared to the OMA systems while maintaining user fairness also. NOMA can be fundamentally divided into two sectors: power domain NOMA and code domain NOMA.

### 2.3.1 Power domain NOMA

Power domain NOMA (PD-NOMA) has attained the most popularity among all the NOMA techniques. This operates by assigning different power levels to several signals of different channel quality with same frequency-time-code resources. Power domain has not been utilized by the ongoing techniques. NOMA superposes multiple signals from different users in power domain and the resultant signal is transmitted over the same frequency resource. The popular superposition coding (SC) is used to do this task [9, 11]. Generally, it assigns higher level of power to the users with weaker channel condition and lower power to the user with stronger channel gain. The receiver adopts an appropriate multiuser detection (MUD) algorithms to detect the signals. SIC is a well admired interference cancellation method in this case [7]. This thesis work basically works with power domain NOMA.

### 2.3.2 Superposition coding

SC in NOMA superposes signals of multiple users over the same resource block (RB). Thus, SC enhances the capacity of NOMA network without the need of en-

larged bandwidth. All the users have access to the available set of resources in NOMA. PD-NOMA implements SC by assigning different power levels to the superposed signals basing on the channel gain of the users. Consider a k-user single cell downlink NOMA network with one base station and all the UE having single antenna are having different channel conditions $(h_1, h_2, ..., h_K)$ where the users are arranged in the ascending order of channel gain $(h_1 < h_2 < h_3... < h_k)$. The network is assumed to experience Rayleigh fading where the $k^{th}$ user has the worst channel gain. The transmitter transmits all the signals superposed by SC from BS to both the users as

$$s = \sum_{k=1}^{K} \sqrt{P_k} x_k \tag{2.1}$$

where, $x_k$ be the signal with $P_k$ transmit power of user $k$ where the transmission power is constrained by $\sum_{k=1}^{K} \sqrt{P_k} = P_{total}$. This total transmission power is fixed beforehand and is divided among the users as per the adopted power allocation (PA) strategy. The received signal turns out to be

$$y_k = h_k s + n_k \tag{2.2}$$

where, $h_k$ is the channel gain of $k$-th user and $n_k$ be the additive white gaussian noise (AWGN) with zero mean and variance $\sigma_n^2$. So, each user receives other users' signal along with its own signal. The assigned power difference in signals help to distinguish the signals for the respective user

### 2.3.3 Successive interference cancellation

SIC is the mostly proposed interference cancellation scheme for NOMA receivers. It helps the receiver to distinguish its own signal from the received signal. SIC operates by treating the signal with better channel condition as noise by the users with weaker channels and decodes its own signal. This happens because the weaker channel signals are provided with higher power than the stronger channel signals. However, the users with better channel gain applies SIC in receivers. First, it decodes the signal of users with weaker channels and then subtracts it from the received signal to finally decodes its own signal.

The received signal from the equation 2.2 is received by all the UE. SIC being used to cancel the interference and decode the signal of $k^{th}$ UE with data rate $R_k$ for

unit transmission BW is be given by

$$R_k = \log_2 \left( 1 + \frac{(P_k |h_k|^2}{|h_k|^2 \sum_{j=k+1}^{K} P_j + \sigma_n^2} \right) \tag{2.3}$$

The data rate of $K^{th}$ user is expressed as

$$R_K = \log_2 \left( 1 + \frac{(P_k |h_k|^2}{\sigma_n^2} \right) \tag{2.4}$$

The achievable sum-rate is $R_s = \sum_{k=1}^{K} R_k$. From equation 2.3 and 2.4 it can be observed that, power allocation scheme can deeply impact the individual data rate and thus, the achievable sum-rate of the system. The downlink PD-NOMA has made it to the 3GPP, which is standardized as multi-user superposition transmission (MUST) [6].

### 2.3.4 Code domain NOMA

Code domain NOMA (CD-NOMA) attains non-orthogonality in code domain. It employs some unique spreading sequences basing on some codebooks or interleaving patterns while sharing the same resources (time, frequency) transmit signals. Its operation is very similar with one OMA system i.e. CDMA. Unlike CDMA, CD-NOMA avails the spreading sequences that are limited to low-density sequence or non-orthogonal low correlation sequences. Based on this, CD-NOMA is categorized as low density spreading (LDS) CDMA (LDS-CDMA), LDS based OFDM (LDS-OFDM) and sparse code multiple access (SCMA).

LDS-CDMA uses sparse coding sequence i.e. the spreading sequence has lesser number of non-zero elements than the conventional one which turns to accumulate more users than the orthogonal one with lower interference [16]. LDS-OFDM is a combination of OFDM and LDS-CDMA where the signal is spread across LDS and then transmitted via a set of sub-carriers. So, basically it is using LDS for multiple access while OFDM for modulation [64]. SCMA is another version of LDS-CDMA but it can directly assign sparse sequences to the data. It assures reduced complexity in receivers and improved performance.

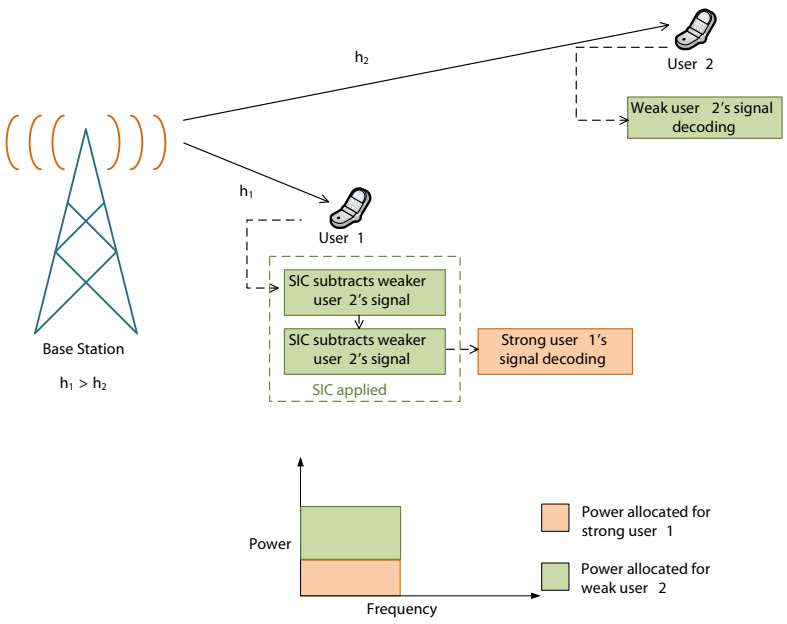


**Fig. 2.1.** A two user single cell NOMA network.

### 2.3.5 Other NOMA schemes

In addition to the popular PD-NOMA and CD-NOMA scheme, some alternative approaches of NOMA are also coming into discussions. Pattern division multiple access (PDMA), multi-user shared access (MUSA), spatial division multiple access (SDMA) are some other NOMA schemes. PDMA employs non-orthogonal sequences or patterns in a way which increases the diversity and reduces overlapping of multiple users [65]. Then it is multiplexed in code or power domain. PDMA enhances the overall performance and error performance due to the diversity [66]. The modulated symbols in MUSA are coded by some sequences specially designed for SIC reception. A huge range of sequences are offered which also may be non-binary. Orthogonal sequences can also be used in MUSA besides the non-orthogonal one. SDMA is another popular NOMA approach where the users are distinguished by the channel impulse responses (CIR) of users. SDMA is mostly helpful when the receiver antennas of BS fall short to the number of uplink users [65]. It would be worth mentioning that we would work in power domain in our thesis work.

### 2.3.6 NOMA in single cell wireless network

A single cell downlink NOMA consists of one BS and $K$-UE with different channel gain. The $K$ different signals are superposed and transmitted non-orthogonally i.e.

same frequency resource is used with a different power level. A 3-UE downlink NOMA network is shown in fig 2.1 with channel gain $h_1$, $h_2$ and $h_3$ where $UE_1$ gets the best channel condition $h_1$ and $UE_3$ receives the worst channel gain $h_3$. PA algorithm is chosen such that $UE_1$ is allotted lowest power and $UE_3$ with highest power to facilitate SIC reception as well as the weak users' performance. Thus, the far UE will experience lower interference than the near UE. The near UE, experiencing higher interference, can smoothly bring out their own signals implementing SIC due to the strong channel gain. The transmitted superposed signal turns out to be

$$s = \sqrt{P_1}x_1 + \sqrt{P_2}x_2 + \sqrt{P_3}x_3 \tag{2.5}$$

where, $x_1$ be the signal with $P_1$ transmit power of user 1 where the transmission power is constrained by $P_1 + P_2 + P_3 = P_{total}$. The received signal to each UE can be represented as

$$y_k = h_k s + n_k \tag{2.6}$$

where, $h_k$ be the channel response of $k$-th UE and $n_k$ be the noise received along with interference.

### 2.3.7 NOMA in multi cell wireless network

In multi-cell downlink NOMA network, several cells with single BS and users co-exist. A multi-cell wireless network consists of two types of UE i.e. UE near the BS are called cell interior (CI) users and UE far from its own BS are called cell edge (CE) users. The CE users face huge ICI from the adjacent cells. A multi-cellular NOMA network is shown in figure 2.2.

An M-cell downlink NOMA is considered with one BS and K-users in each cell. The system BW B is divided into N sub-bands in each cell. User pairing is achieved basing on their channel conditions i.e. CI users are normally paired with CE users because of their asymmetric channel gain which facilitates SIC reception. For the $l$-th user index at sub-band $\varphi$ ($\varphi \in N$), the transmitted signal $x_\varphi$ for the transmitted symbol $s_\varphi(u_\varphi(l))$ of the $u_\varphi(l)$-th user can be expressed as

$$x_\varphi = \sum_{l=1}^{n_\varphi} \sqrt{P_\varphi(u_\varphi(l))} s_\varphi(u_\varphi(l)) \tag{2.7}$$

where, $p_\varphi(u_\varphi(l))$ is the power coefficient for the user $u_\varphi(l)$ at sub-band $\varphi$, $n_\varphi$ is the number of users scheduled on sub-band $\varphi$ and $E[|s_\varphi(u_\varphi(l))|^2] = 1$. The received

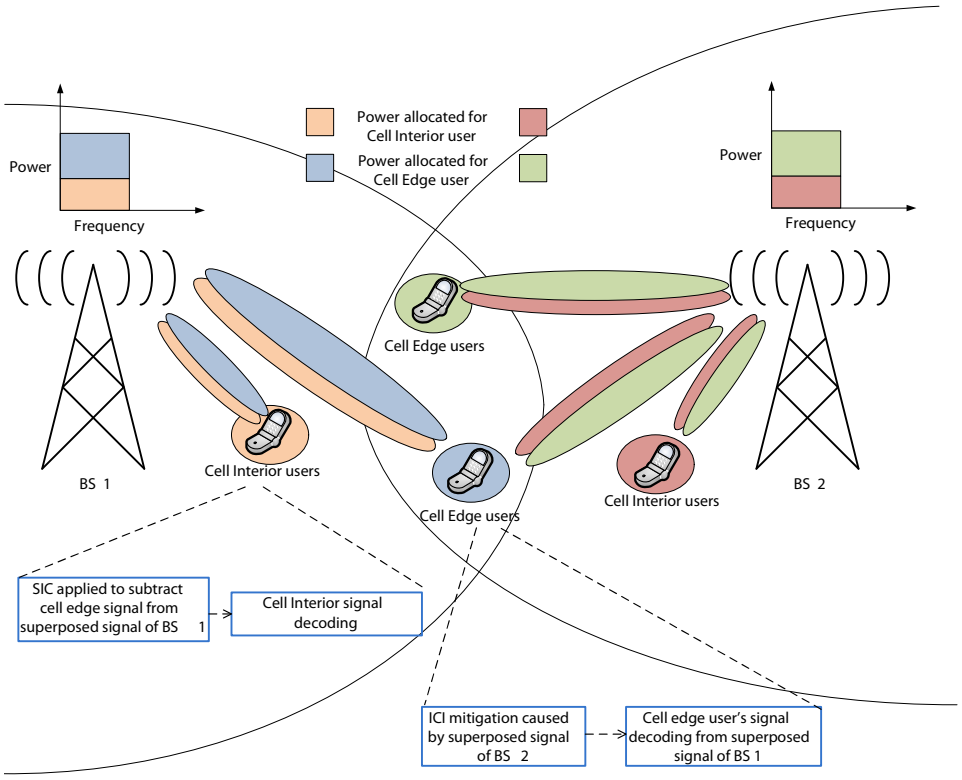


**Fig. 2.2.** A multi-cell NOMA scenario.

signal $y_\varphi(u_\varphi(l))$ of the $u_\varphi(l)$-th user is

$$y_\varphi(u_\varphi(l)) = h_\varphi(u_\varphi(l))x_\varphi + w_\varphi(u_\varphi(l)) \tag{2.8}$$

where, $h_\varphi(u_\varphi(l))$ is the channel gain of user $u_\varphi(l)$ and $w_\varphi(u_\varphi(l))$ is the noise and ICI of user $u_\varphi(l)$ at sub-band $\varphi$.

## 2.4 Comparative Study between OMA and NOMA

While OMA technologies are lagging behind to achieve overall sum-rate capacity of multi-user communication, NOMA chalks out several ways to attain the achieve sum-rate requirement of multi-user communication.

OMA techniques have gradually enhanced its capacity over the time through different generations in cellular communication. But the number of users is still limited by the number of available orthogonal resources in OMA. Also, despite using orthogonal resources (frequency, time or code), the channel-induced impairments nearly destroy their orthogonality.

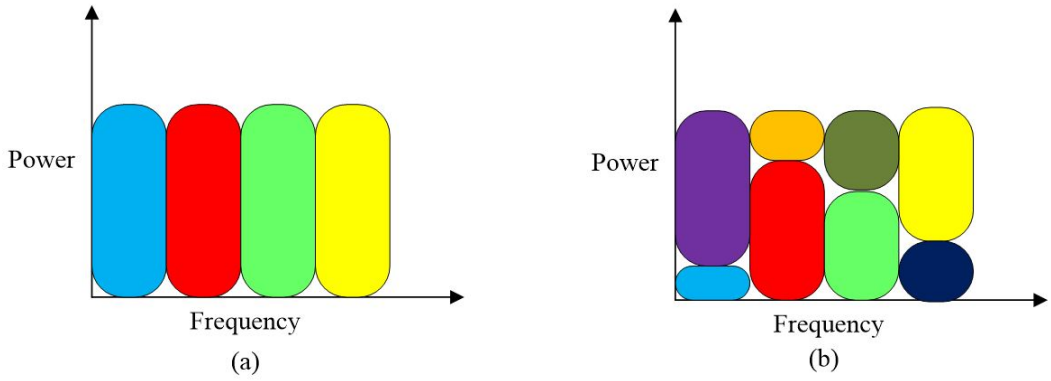


**Fig. 2.3.** Pictorial representation of the difference between OMA and NOMA operation. The resources of (a) OMA and (b) NOMA operation is colored differently.

OMA basically focuses on the strong users with better channel condition and assigns all the resources to it in order to enhance the overall system performance. However, this scenario overlooks the performance of users with weaker channel gain. The weaker users, thus, have to wait to be served in time domain OMA. This introduces high unfairness and increased latency. NOMA, on the other hand, is capable of ensure fairness among users. It maintains a balance in allocating resources between the paired users which, in turn, facilitates the weak users. Moreover, it can serve several users simultaneously with the same time-frequency resources, so no users have to be in the queue to be served resulting the latency to be lessened appreciably.

Due to the orthogonal resource assignment, OMA users face no interference while receiving signal. Thus, the OMA receivers do not have any additional features and the receiver complexity is lower than NOMA receivers. Interference is ever-present in NOMA because several users are served over the same sub-carrier. NOMA receivers must have arrangements to detect and receive the signals from the superposed signal over the same sub-carrier. This increases the complexity of NOMA receivers.

A huge challenge for NOMA in 5G is to maintain the energy efficiency (EE), because NOMA is offering the assemblance of huge devices which tend to enhance the energy consumption extensively. So NOMA adopts several strategy to balance between achieving SE and optimum EE. A comparative study between OMA and NOMA is shown in table 2.1. NOMA is seen to provide better SE, user fairness and lower latency at the cost of slightly increased receiver complexity than OMA. These features make NOMA appealing to adopt for 5G and beyond.

**Table 2.1:** Comparison Between OMA and NOMA Scheme.

| MA Technique | Advantages | Disadvantages |
|---|---|---|
| OMA | • No interference<br>• Simple receiver design | • Restriction in connectivity<br>• Increased latency<br>• Unfair scheduling of users<br>• Lower SE |
| NOMA | • Higher SE<br>• Bulk connectivity<br>• Lower latency<br>• Improved user fairness | • Presence of Interference<br>• Increased receiver complexity |

## 2.5 Conclusion

This chapter gives an idea of several MA techniques and their evolution over the different cellular generations. The idea of basic NOMA operation both in power domain and code domain is discussed. This thesis will further discuss about power domain NOMA. The received and transmitted signal pattern for both single cell and multi cell NOMA are analyzed and explained. Finally, the overall pros and cons of OMA and NOMA are studied and thus, this work will advent further with NOMA in the upcoming chapters because of its exciting features which completely merge with 5G requirements. The next chapter will discuss the other 5G features which can be incorporated with NOMA for an even better performance.

# CHAPTER 3

# INCORPORATION OF OTHER 5G FEATURES

## 3.1 Introduction

In order to get rid of the connectivity restriction imposed by 4G, 5G is offering many unique features to serve this giant number of IoT devices. 5G is expected to have about 1000 times more capacity, 100 times more data rates and low latency lesser than 1 ms [67] than 4G-LTE networks. These requirements will be fulfilled only by the accumulation of the 5G techniques. Beamforming, massive MIMO, mmWave are some promising technologies that are being offered by 5G besides NOMA [4] to cope up with this demand of massive connectivity.

## 3.2 Millimeter Wave Communication

mmWave communication has been accepted to be a strong candidate among the 5G features to enhance the network capacity by extending the existing bandwidth (sub 6 GHz) spectrum [68]. The large spectrum at mmWave band (30-300 GHz) was not utilized for mobile communication till 4G-LTE network. This unutilized high frequency spectrum will improve the throughput gains significantly [69] by ranging the data rate up to gigabits per second. Another exciting feature of mmWave is providing low latency which also is a prime requirement of 5G [70]. But mmWave creates severe path loss due to its shorter wavelengths which can be overlooked by the benefits of wide range of bandwidth. The shorter wavelength of mmWave brings the concept of large antenna arrays at both the BS and the receivers [pd or switch]. Also, the path loss can be avoided by the directional beams of these large arrays of antennas [71]. This facilitates the concept of multi user multiple-input multiple output (MU-MIMO) to massive MIMO.

## 3.3 Massive Multiple-Input Multiple-Output

MIMO is another exciting feature to enhance the spectral efficiency of both the microwave and mmWave wireless channels [72]. The MIMO concept enables the number of antenna elements at BS to reach to several users with multiple antenna. MIMO evolves into massive MIMO delivers reliable communication by enhancing capacity and offering high data rates. The integration of mmWave and massive MIMO will act as capacity boosters because of the extended bandwidth and higher spectral efficiency [5]. But, massive MIMO engenders excessive transceiver complexity and energy consumption because each antenna in MIMO systems usually requires one dedicated radio-frequency (RF) chain [73] each of which consists of the power consuming phase shifters (PSs), digital-to-analog converter (DAC) and analog-to-digital converter (ADC). So, the huge RF chains caused by the use of an equally huge number of antennas in mmWave MIMO systems will lower the energy efficiency extensively. The approximation says that RF components may absorb up to 70% of the total transceiver energy consumption [74]. Thus, massive MIMO becomes unaffordable in practice due to the high hardware cost and energy absorption. The only way to utilize the benefits of MIMO is by reducing the number of the power-hungry RF chains. This inspires the enhancement of new transceiver architectures in MIMO.

## 3.4 Beamforming

Beamforming with a large antenna array is used to diminish path losses caused by mmWave communication with directional transmissions [75]. Beamforming lowers the amount of path loss caused by the mmWave transmission through its directional beams and lowers the amount of interference also.MIMO with multi-user beamforming is a promising sector to elevate the overall system throughput. Each user of multiple antenna is served by single or multiple beams basing on the number of transmit and receive antennas at BS and users respectively. The inter-beam interference can be avoided in case of equal or more BS antennas than the receive antennas. Each beamforming gain of a user is orthogonal to the other receivers' beamforming gain. But, the conventional beamforming system (digital beamforming), though offers better SE, becomes unacceptable because of using the large number of RF chains as the number of antennas [71]. Analog beamforming, however, transmits single data streams only using one RF chain and several phase shifters. Thus, hybrid analog/digital beamformers are proposed which can provide better SE like digital beamforming but at

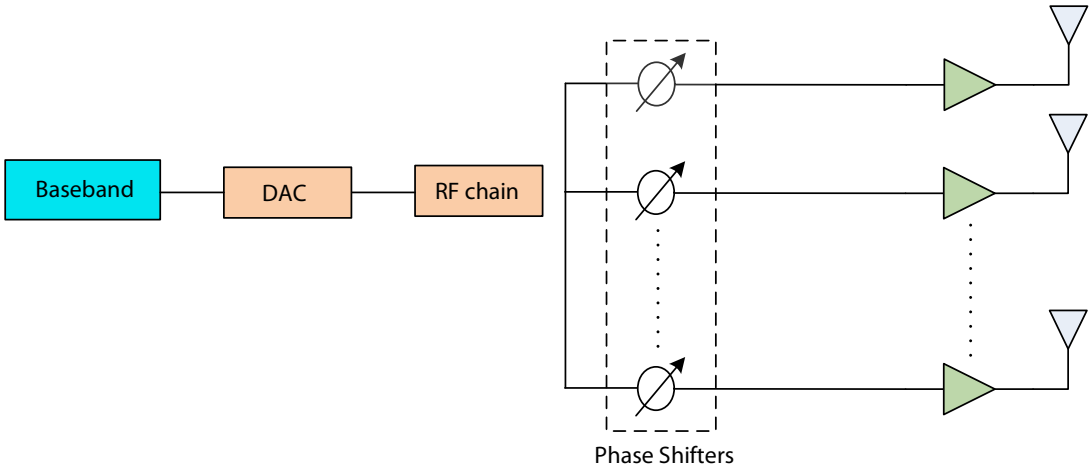


**Fig. 3.1.** Analog beamforming at the BS.

reduced hardware complexity.

### 3.4.1 Analog beamforming

Analog beamforming structure (ABS) offers much reduction in cost by dedicating one RF chain with several PSs. Analog beamformer employs analog phase shifters which alters the phases of the signals and directs the signal beam to the desired directions. It absorbs high power and cannot provide multiplexing of the data streams. Analog beamforming is an approach that relies entirely on RF domain processing to reduce the number of RF chains. Ultimately, the performance of analog beamforming is limited by quantization of the phase angles and the support of only single stream MIMO transmission.

### 3.4.2 Digital beamforming

Digital beamforming structure (DBS) requires one RF chain per antenna element at both the transmitter and receiver. A typical RF chain contains low-noise amplifier, DACs, ADCs, down-converter etc [72]. So, for the large number of antenna array elements, the cost and energy consumption become so large that it becomes unrealistic to use one RF chain per antenna. For these reasons, beamforming structure with limited number of RF chains has recently received significant attention. One approach of achieving this goal is to deploy beamforming at both the digital and analog domains, i.e., hybrid beamforming structure.

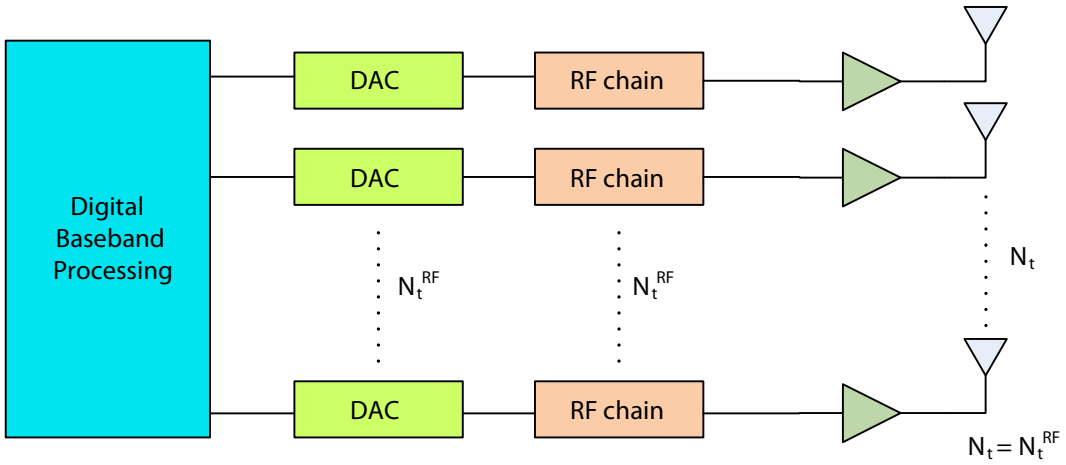


**Fig. 3.2.** Digital beamforming at the BS.

### 3.4.3 Hybrid beamforming

Employing a fully DBS MIMO turns out to be impractical because of its low energy efficiency and high cost. However, the combination of analog beamformers with digital beamforming brings about the concept of hybrid beamforming structure (HBS) which offers a promising solution of these problems where MIMO processing is divided between the analog and digital domain [70]. The reduced number of RF chains combines the low-dimension digital precoder and high-dimension analog precoders. The analog precoder being of high dimension, it should not be implemented in the RF chains with the energy consuming components [76]. Thus, the analog precoders are always implemented with low expense PSs which makes them incapable to change the magnitude of RF signals. The digital precoder makes it possible to enable multi-user transmission. HBS can transmit multiple data by saving the cost and reducing the hardware complexity as well as energy consumption by lowering the number of RF chain in massive MIMO system [77].

HBS can be classified in two types of architecture: fully connected structure (FC-HBS) and sub-connected structure (SC-HBS). In FC-HBS, all the RF chains are connected to all the antennas which increases the hardware complexity. A FC-HBS is shown in fig. 3.4. FC-HBS enables more PSs in the analog domain than the other structures. Thus the use of large-scale PS will increase the complexity and the power consumption [78] which could be a hurdle for the resource constrain of IoT. But the SE of FC-HBS can approach upto the DBS performance in mmWave

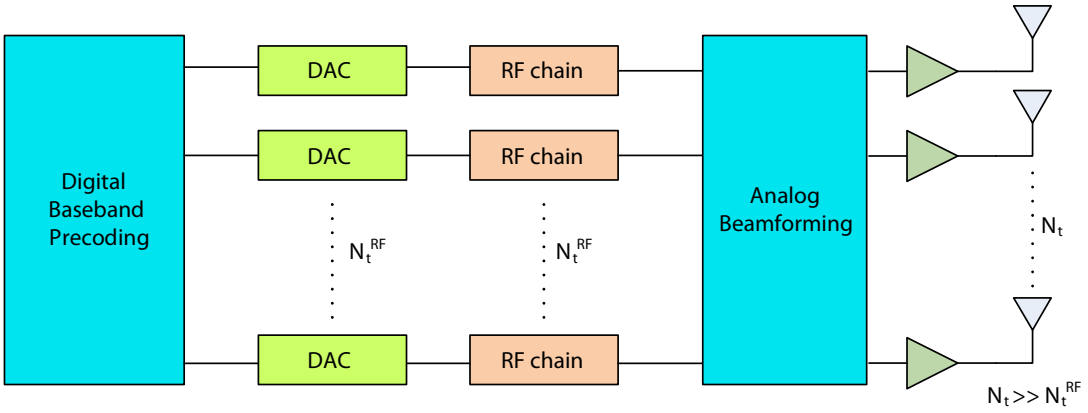


**Fig. 3.3.** Hybrid beamforming.

channels [79]. In SC-HBS, as shown in fig. 3.5 each RF chain is connected to a sub-array of antenna elements only which makes the set-up less complex than the former one. But it provides lower beamforming [79] gain and thus, FC-HBS ensures better performance than SC-HBS at the cost of largely increased complex structure and energy consumption.

## 3.5 Proposed Beamforming Design

To overcome these challenges of FC and SC structure, various type of suboptimal energy hardware efficient HBS with PS has been proposed. In this thesis, we propose fuzzy based energy efficient HBS (FeE-HBS) architecture with PSs. The fuzzy based switching enables less PSs when the requirement is less. This makes the system more dynamic and lessens the power consumption of the network. Thus the proposed system reduces the hardware complexity of the network to a great extent, improves the energy efficiency and delivers desirable data rates. The main aim is to improve the overall system performance of the hybrid-mmWave-massive MIMO systems.

The proposed system model has one BS equipped with $N_t$ antennas and $N_t^{RF}$ number of RF chains such that, $N_t >> N_t^{RF}$. The $N_S$ data streams are being transmitted from the antenna array of the BS to users each with $N_r$ antennas ($N_r = N_t$) and $N_r^{RF}$ RF chains. Proposed FeE-HBS model is illustrated in fig. 3.6. In the transmitter section, there are main three subsystems: digital precoder, RF chain and fuzzy based analog precoder. The base band signal is processed by $N_t^{RF} \times N_S$ dimensional digital precoder, then converted into $N_S \times N_t^{RF}$ dimensional RF signal using RF chain. The RF chains are coded with fuzzy based analog precoder. The output of the RF chain

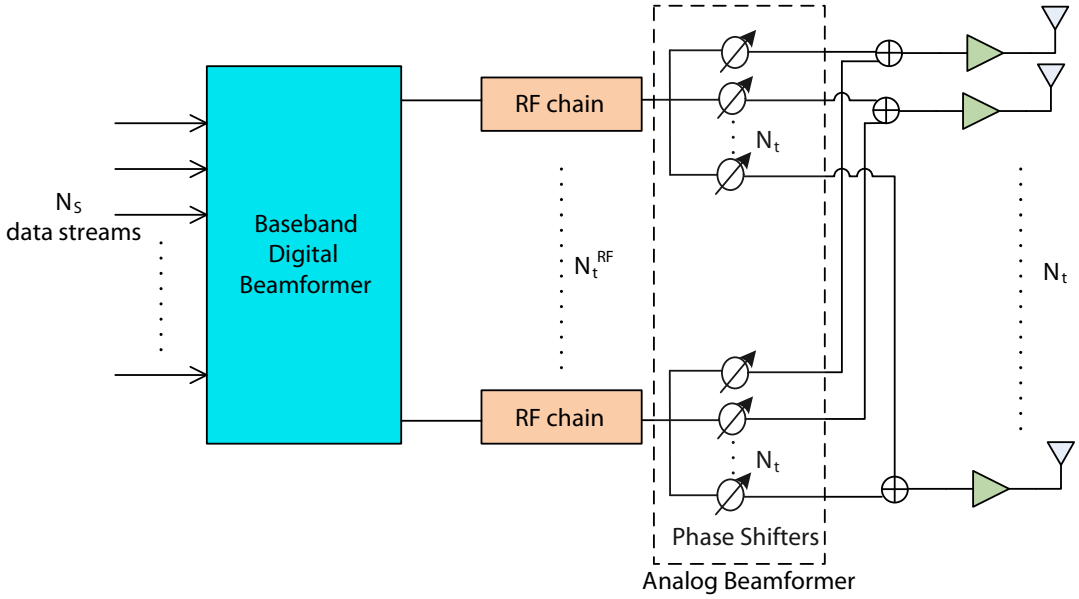


**Fig. 3.4.** Fully connected hybrid beamforming.

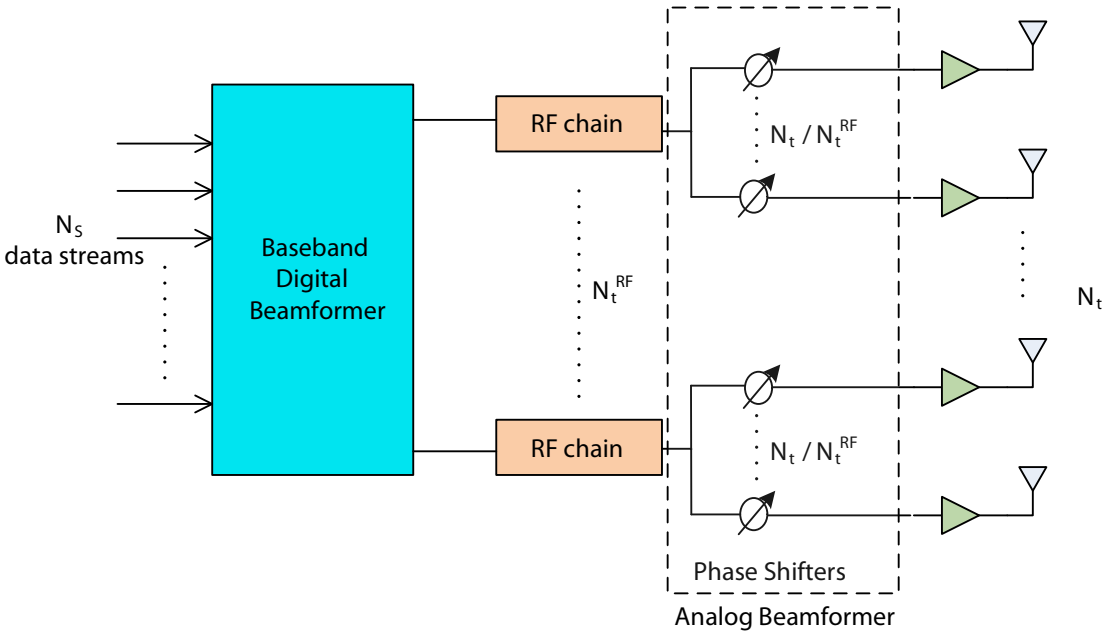


**Fig. 3.5.** Sub-connected hybrid beamforming.

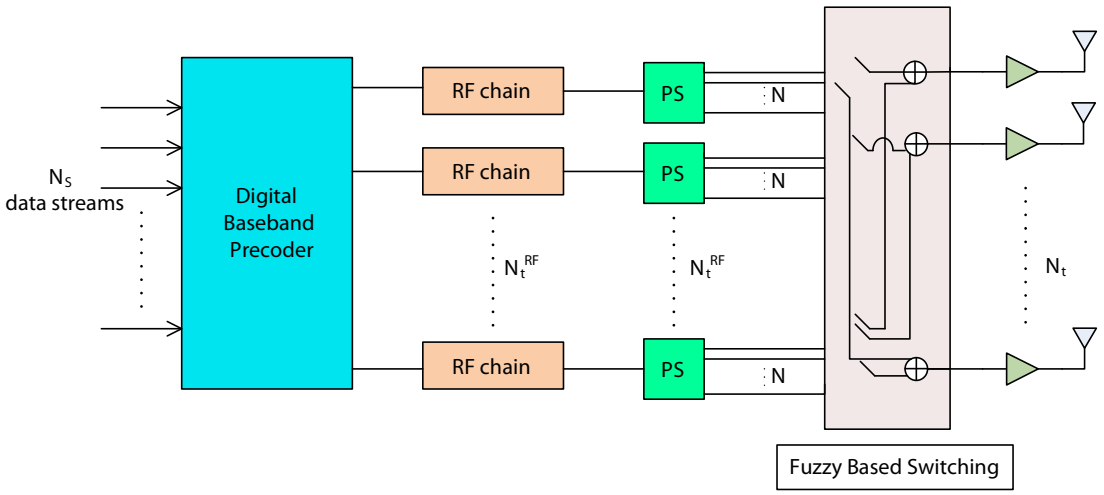


**Fig. 3.6.** Proposed FeE-HBS system model.

is fed into PSs for generating $N$ parallel signals with same amplitude $1/\sqrt{N}$ and different phases. Finally, the signal with required phase will be fed into fuzzy based switching matrix for transmitting with MIMO antenna array. The transmitted signal can be expressed as

$$x = \mathbf{F}s \tag{3.1}$$

where, the hybrid precoding matrix $\mathbf{F} = \mathbf{F}_{AB}\mathbf{F}_{DB}$ is applied to transmitted symbol vector $s = \begin{pmatrix} s_1 & s_2 & \dots & s_{N_S} \end{pmatrix}^T \epsilon\ \mathcal{C}^{N_s \times 1}$ in the baseband with $\mathbb{E}\left[ss^H\right] = I_{N_s}$. $\mathbf{F}_{DB}$ be an $N_t^{RF} \times N_t$ baseband digital precoder matrix. For FC structure where the data streams are connected to all RF chains, $\mathbf{F}_{DB}$ is expressed as

$$\mathbf{F}_{DB} = \begin{pmatrix} d_{11} & \cdots & d_{1N_s} \\ \vdots & \ddots & \vdots \\ d_{N_t^{RF}1} & \cdots & d_{N_t^{RF}N_s} \end{pmatrix} \tag{3.2}$$

But we consider the SC structure where single RF chain is connected to each data stream. This reduces $\mathbf{F}_{DB}$ to a diagonal matrix $\mathbf{F}_{DB} = diag\left(d_{11}, d_{22}, \dots, d_{N_t^{RF}N_s}\right)$. The digital precoded data is directly fed into the analog beamformer of the corresponding sub-array. $\mathbf{F}_{AB}$ be the $N_S \times N_t^{RF}$ analog beamforming matrix which can be expressed as

$$\mathbf{F}_{AB} = \begin{pmatrix} a_1 & 0 & \dots & 0 \\ 0 & a_2 & \dots & 0 \\ \vdots & \vdots & \ddots & \vdots \\ 0 & 0 & \dots & a_{N_t^{RF}} \end{pmatrix} \tag{3.3}$$

We consider the frequency-flat channel for narrowband frequency. Assuming the widely accepted Saleh-Valenzuela channel model for L number of paths, the channel matrix $\mathbf{H}\ \epsilon\ \mathcal{C}^{N_r \times N_t}$ can be expressed as

$$\mathbf{H} = \gamma \sum_{l=1}^{L} \alpha_l \mathbf{a}_r(\phi_l^r)\mathbf{a}_t^H(\phi_l^t) \tag{3.4}$$

where $\alpha_l$ is the complex gain for $l^{th}$ path with $\mathbb{E}\left[|\alpha_l|^2\right] = 1 = 1$ and $\gamma$ is a normalization factor. $\phi_l^r \epsilon\, [0, 2\pi]$ and $\phi_l^t \epsilon\, [0, 2\pi]$ are the $l^{th}$ paths angle of departure (AOD) and angle of arrival (AOA) respectively. $\mathbf{a}_r(\phi_l^r)$ and $\mathbf{a}_t^H(\phi_l^t))$ be the array response vectors of BS and user respectively. Considering uniform linear array (ULA), $\mathbf{a}_t(\phi_l^t))$ can be expressed as

$$\mathbf{a}_t(\phi_l^t) = \frac{1}{\sqrt{N_t}} \left[1, e^{j\frac{2\pi}{\lambda} d \sin\phi_l^t}, \dots, e^{j(N_t-1)\frac{2\pi}{\lambda} d \sin\phi_l^t}\right] \tag{3.5}$$

Then the received signal will be

$$\mathbf{r} = \sqrt{\beta}\mathbf{H}\mathbf{F}\mathbf{s} + \mathbf{n} \tag{3.6}$$

where $\beta$ be the power coefficient and $\mathbf{n}\ \epsilon\ \mathcal{CN}(0, \sigma^2)$ be the AWGN vector. The user combines the received signal via a hybrid combiner $\mathbf{W} = \mathbf{W}_{AB}\mathbf{W}_{DB}$ where $\mathbf{W}_{AB}$ be the analog RF combiner and $\mathbf{W}_{DB}$ is the digital combiner. So, the received signal after processing is

$$\mathbf{y} = \sqrt{\beta}\mathbf{W}^*\mathbf{H}\mathbf{F}\mathbf{s} + \mathbf{W}^*\mathbf{n} \tag{3.7}$$

### 3.5.1 Switching algorithm

In our FeE-HBS system, the signal with required phase will be fed into Fuzzy based switching matrix for transmitting with MIMO antenna array. This switching is designed which aims to maximize the sum rate. The performance of precoder and switching matrix system depends on selection of appropriate PSs. However, optimal

search algorithm increases the complexity of the HBS. The fuzzy based low complexity design requires to compromise with the performance of the HBS. Chafaa et al. [80] and Peng el al. [81] proposed estimation of mmWave channel parameters such as: the path gain, the AOA and AOD. In this work, we have considered that the CSI information are available at the receiver as per these estimation techniques. In addition, AoD of a group of uses takes values from $[0, 2\pi]$ whereas the mean AoA of a group follows uniform distribution over $\pi/3$ sector. Fig. 3.7 shows fuzzy logic controller (FLC) for the switching matrix operation. Based on the fuzzy inference rules, FLC may select PS to be switched on considering differentiation of AoA, AoD and data rate demand. Each variable contains three linguistic terms low (L), medium (M) and high (H) and they follow gaussian membership function. The relation between the input and output membership functions is shown in fig. 3.7.

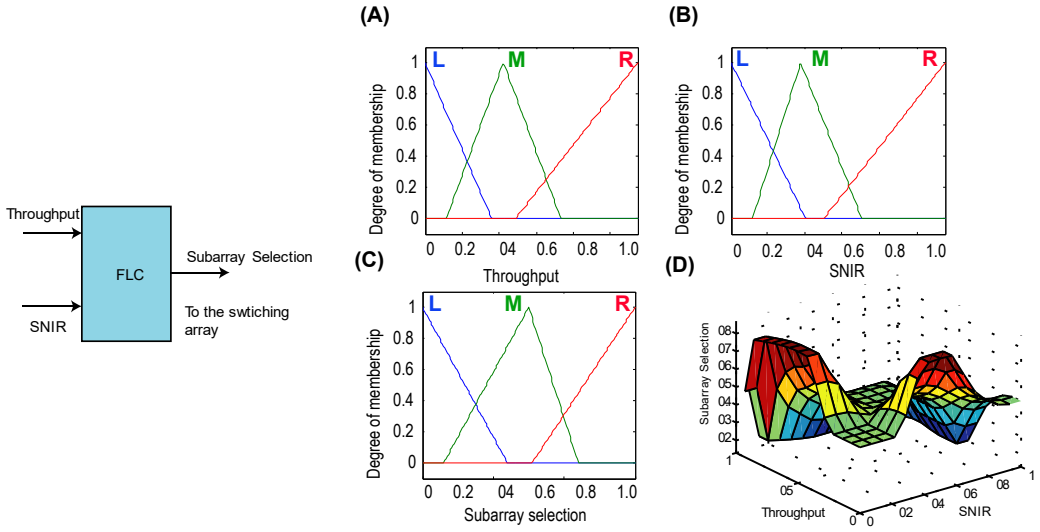


**Fig. 3.7.** Fuzzy logic controller selects subarray of the mmWave antenna (top) whereas subarray selection is a function of throughput and signal to noise plus interference ratio. The bottom figure shows the surf plot of the input and output membership functions.

## 3.6 Conclusion

Beamforming facilitates the MIMO transmission enormously. Though digital beamforming offers a grater amount of SE, it is not practical to afford the complex energy consuming structure. Hybrid beamforming can provide a moderate performance at less complexity. FC-HBS offers better performance at more complex structure whereas the SC-HBS provides just the opposite i.e. lower SE than FC structure with

higher energy efficiency. So, a novel FeE-HBS for mmWave massive MIMO system is proposed which lowers the number of PS per sub-array than the traditional FC structure to deal with the energy consumption of analog PS. Moreover, the adoption of a Fuzzy based switching network makes the architecture more dynamic compared to the conventional SC-HBS. The switching helps to select PSs as per one's criteria. This enables the propose FeE-HBS system to achieve higher energy efficiency at desirable spectral efficiency than the conventional hybrid structures. In the next chapter, we will explore new ways to achieve lower inter cell interference to further enhance the performance of the network.

# CHAPTER 4

# FREQUENCY REUSE TECHNIQUES

## 4.1 Introduction

5G focuses on enhancing the data transmission rates, bulk connectivity and improved quality of service (QoS). But severe path loss, signal attenuation by high frequency signals and the interference from the neighboring cells create major obstacles in achieving these requirements. The ever-increasing demand of 5G leads to incorporate huge nodes in each cell to achieve higher SE. Consequently, this accumulation of large number of devices had made the interference management (IM) a prime issue in the way of achieving higher capacity of the wireless networks. Several IM techniques are adopted by both OMA and NOMA networks to avoid the interference [22, 53, 54, 56, 82]. The intra-cell interference is tackled by assigning orthogonal resources in OMA and applying SIC in the NOMA receivers. But inter-cell interference (ICI) from neighboring cells is still present in multi-cellular NOMA networks[56]. In fact, it is the prime source of interference in OFDMA networks also. ICI creates a major hindrance in the way of achieving higher SE both in OMA and NOMA networks. Both OMA and NOMA adopted various interference mitigation techniques to alleviate the ICI.

## 4.2 Inter-Cell Interference Mitigation Techniques

ICI is the interference among the user nodes of neighboring cells which use the same frequency in different cells. It results into severe performance degradation of wireless networks. Generally, ICI is handled by any of three major ways: randomization, cancellation and avoidance or coordination. Randomization of ICI does not enhance edge node's performance which is a major concern for us. ICI cancellation techniques cancels interference at the cost of increasing receiver's computational

complexity to a great extent. ICI avoidance or coordination technique employs its resources such a way that it does not interfere. It leads to the efficient management of the system bandwidth.

Frequency reuse falls in this category of interference mitigation. It can be a better tool to reduce the ICI [83], especially to the edge users. They can mitigate the ICI by providing particular rules on the sub-band assignment and power allocation without degrading the system performance [50]. Adjacent cells are assigned different sub-carriers in frequency reuse techniques in a way that they do not interfere with each other at the cost of reduced bandwidth efficiency. Fractional frequency reuse (FFR), soft frequency reuse (SFR), sectored FFR are some frequency reuse techniques which enhance capacity by utilizing two separate frequency reuse factors (FRF) instead of a single one. Hard frequency reuse, on the other hand, divides the bandwidth as per the FRF which is same for CI and CE users. No adjacent cells can use the same frequency thus do not face any interference in hard frequency reuse [84] which is shown in fig. 4.1(a). This affects the bandwidth efficiency severely.

## 4.3 Fractional Frequency Reuse

The motto behind adopting any reuse technique is to keep the interference minimum while maintaining a moderate bandwidth efficiency. FFR is such a technique which aims to maintain a balance between achieving high SE and ICI mitigation of edge users [85]. FFR or sometimes termed as strict FFR divides the available bandwidth into interior and exterior sub-bands . A common set of sub-bands is assigned to the interior users near the BS and the exterior bandwidth is partitioned across the cell and distributed to the users in the edge of cells basing on a fixed FRF [52]. Thus it employs different FRF to the cell interior (CI) and cell edge (CE) users since the edge users are generally subjected to more interference. The CI users who have comparatively higher SINR are assigned lower FRF (e.g. $\Delta$=1) than the CE users' FRF (e.g. $\Delta$=3) who have lower SINR. Strict FFR is an effectual solution for ICI mitigation since it focuses on the performance of CE users at the cost of compromising slightly with the overall throughput. A typical FFR with FRF 3 ($\Delta$=3) is shown in fig. 4.1(b). For a reuse factor of $\Delta$ stict FFR requires total $\Delta + 1$ number of sub-bands. FFR scheme can be executed either statistically or dynamically. All the parameters are preassumed and the spectrum is pre-allocated in advance in static FFR. In dynamic FFR scheme, the parameters are subjected to the change of channel and traffic condition [54].

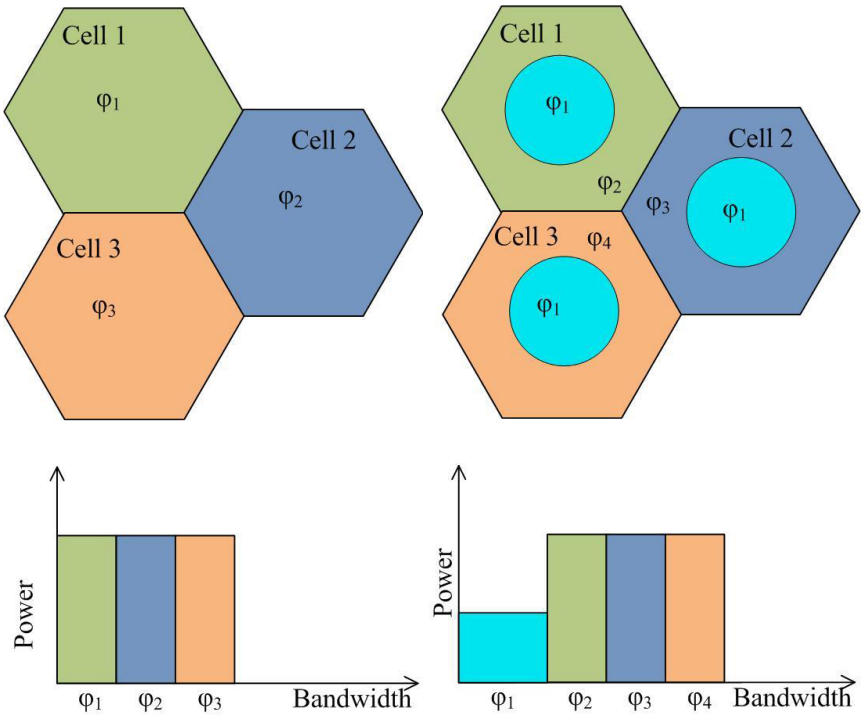


**Fig. 4.1.** (a) Hard frequency reuse-3 (b) Strict FFR with FRF = 3 for the edge users and FRF = 1 for CI users.

## 4.4 Soft Frequency Reuse

Soft frequency reuse is very similar in operation with FFR. It utilizes the same spectrum partitioning as strict FFR but the difference is that, it allows the CI users to share its sub-bands with CE users of different cells [51]. This makes the system bandwidth efficient but with increased ICI. For this reason, the whole bandwidth in each cell is divided into two bands i.e. primary band and secondary band. Primary band used in the cell edge are allotted more power than the secondary in each cell[21]. The secondary band is assigned to the CI users with lower power. This helps in minimizing the ICI. SFR scheme for FRF 3 ($\Delta$=3) is shown in fig. 4.2.

However, FFR assures lesser ICI than SFR by allotting different sub-bands to the CI users from CE users. SFR, on the other hand, ensures the best utilization of the bandwidth by employing all sub-bands in all cells.

## 4.5 Sectored Fractional Frequency Reuse

Sectored FFR is a modification of strict FFR. It employs the same idea of dividing the bandwidth according to an FRF like strict FFR [49]. The use of directional

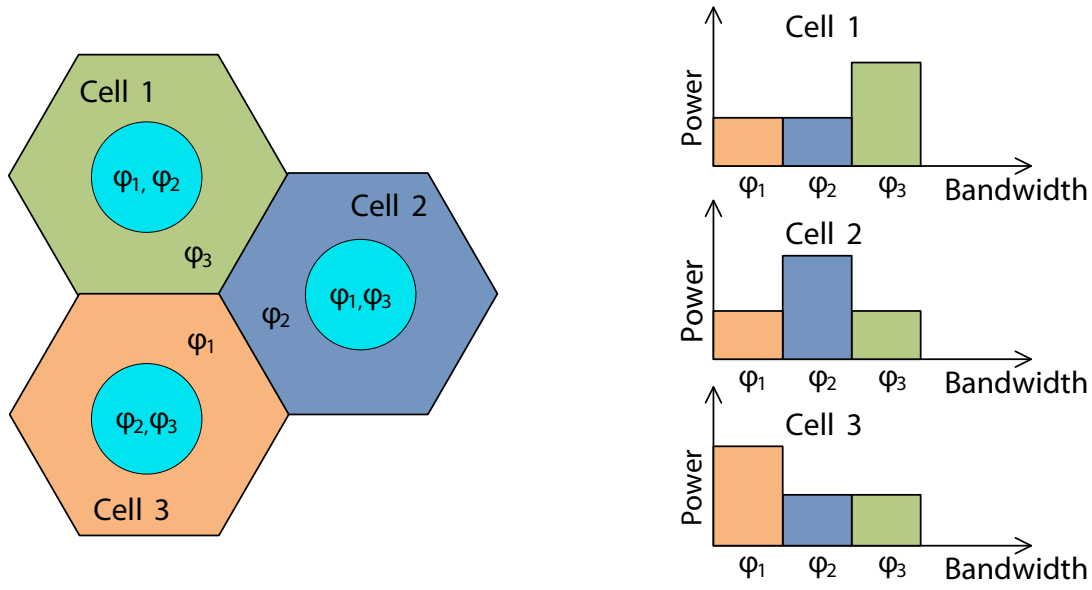


**Fig. 4.2.** SFR with FRF = 3.

antenna for CE users to further minimize the ICI is the promising feature of sectored FFR. Since 5G is incorporating directional antenna with the omnidirectional one, sectored FFR is the choice of interest in our thesis work. The use of directional antenna by sectored FFR results in the decrease of ICI extensively. Sectored FFR combines the benefits of strict FFR and SFR together but at the cost of slightly enlarged system complexity. The system becomes bandwidth efficient because each cell uses all the sub-bands available in the bandwidth like SFR whereas the ICI is still lower than SFR configuration thus offering improved SE than both FFR and SFR. By directing the signals in desired direction only, signal quality increases without the necessity of complex power control as in SFR [55].

### 4.5.1 Conventional sectored FFR

Sectored FFR sectorizes the exterior area of hexagonal cells into sectors and direct a particular set of sub-bands in that sectors. It uses directional antenna for the CE area. The cell interior is not sectorized and thus the omni-directional antenna will work smoothly for the interior sub-band assignment with FRF 1 [86]. Fig. 4.3 shows the 3-sectored FFR where the bandwidth in each cell is divided into four equal set of sub-bands ($\varphi_1$, $\varphi_2$, $\varphi_3$ and $\varphi_4$). The interior area in each cell is employing same sub-bands $\varphi_1$ for the CI area. Each cell BS utilizes tri-sectored antenna to sectorize the

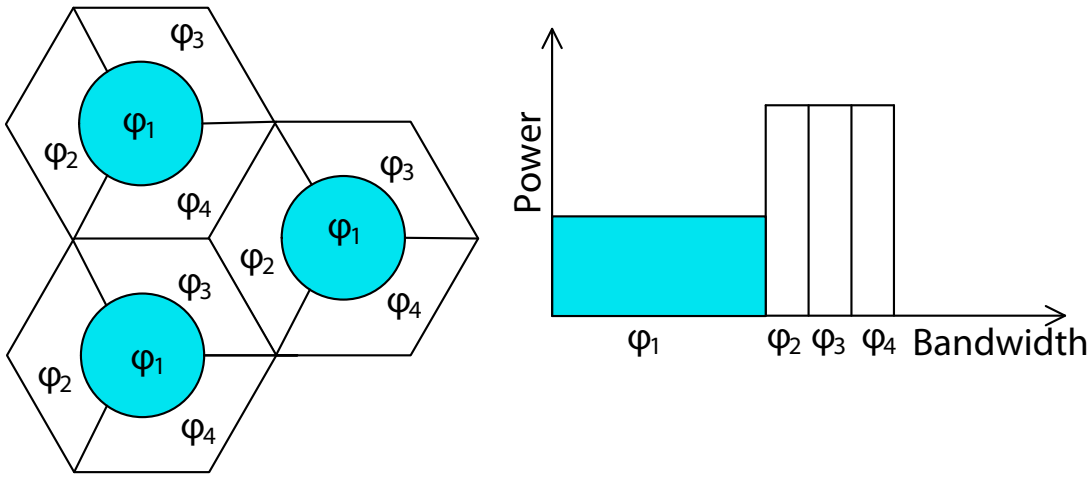


**Fig. 4.3.** Sectored FFR with FRF = 3.

edge area and assign 3 separate sub-bands to them. Thus it divides the bandwidth in $n+1$ number of sub-bands where SFR divides it in $n$ sub-bands for the same FRF (=3).

It utilizes all the sub-bands in all the cells so the bandwidth utilization becomes maximum. Since the CI users sub-band is not reused in the edges, it keeps the ICI lesser than SFR.

## 4.6 Proposed Sectored FFR

Amongst the aforementioned techniques (strict FFR, SFR and sectored FFR), our choice of interest lies in the latter one. Since we are assimilating reuse scheme with NOMA network with directional antenna, sectored FFR is considered to be the right technique for the system.

The proposed 6-sectored model is shown in fig. 4.4. First, the user classification is achieved based on their SINR. Users having SINR less than the fixed threshold SINR are considered as exterior or CE users while users' SINR greater than threshold value is counted as CI users. The total bandwidth is divided in equal sub-bands $\varphi$ which is accessible in each cell. $\varphi$ is again sub-divided such that $\varphi = \varphi_1, \varphi_2, ..., \varphi_n$. All the users in CI are assigned $\varphi_1$ sub-bands in each cells (FRF =1) but not shared with CE users. The rest of the split sub-bands are assigned to the CE users by the directional antenna in a way that the ICI be the minimum. Now the conventional 6-sectored FFR divides the sub-band $\varphi$ in n number of sub-bands ($n = 7$ for conventional 6-sectored

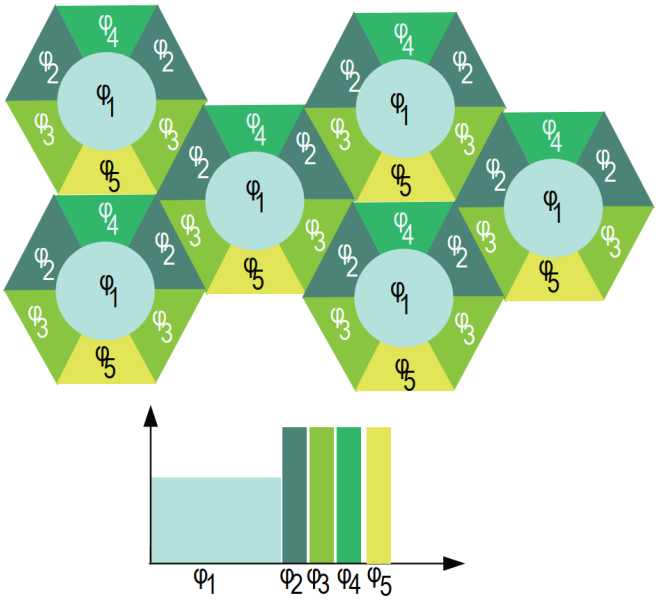


**Fig. 4.4.** Proposed sectored FFR model.

one) whereas our proposed system divides it in $n-2$ ($=5$ in this case) number of sub-bands. This result into the lesser splitting of sub-bands which accumulates more users in each cell which escalates the SE. Since we are using NOMA network, our proposed reuse scheme also facilitates the user grouping while ensuring fairness. Moreover, the directional antenna and sectorization of cells together make a great tool to keep the ICI minimum.

### 4.6.1 System Model

A $W$- cell downlink NOMA system model along with SIC at the receivers is considered. Each BS is designed with single antenna having $K$ users in individual cell and for the system bandwidth $B$ the total set of sub-bands in each cell required to transmit the data streams is $\varphi$ such that, $\varphi = \varphi_1, \varphi_2, ..., \varphi_m$. User pairing is attained by grouping the users in one cell basing on their channel criteria [48]. The CI users which are located close to BS, thus having a better channel gain, say, $h_1$, are usually paired with the CE users far from BS with a poor channel gain, say, $h_2$ ($h_1 > h_2$). Each user is considered to have $N_r$ antennas. The strong users will recover their signals despite being assigned with lower power by applying SIC to the receivers.

The multiuser scheduler assigns the set of users $U_{\varphi_i} = u_{\varphi_i}(1), u_{\varphi_i}(2), ..., u_{\varphi_i}(L)$ at

sub-band $\varphi$ where $L$ is the number of users scheduled at the sub-band $\varphi_i$. For the $l$-th user index at sub-band $\varphi_i$, the transmitted signal $x_{\varphi_i}$ for the transmitted symbol $s_{\varphi_i}$ $(u_{\varphi_i}(l))$ of the $u_{\varphi_i}(l)$-th user can be expressed by using equation (4.1)[56]

$$x_{\varphi_i} = \sum_{l=1}^{L} \sqrt{\beta_{\varphi_i}(u_{\varphi_i}(l))} s_{\varphi_i}(u_{\varphi_i}(l)), \tag{4.1}$$

where, $\beta_{\varphi_i}(u_{\varphi_i}(l))$ is the power coefficient for the user $u_{\varphi_i}(l)$ at sub-band $\varphi_i$ and $E[|s_{\varphi_i}(u_{\varphi_i}(l))|^2] = 1$. The received signal $y_{\varphi_i}(u_{\varphi_i}(l))$ of the $u_{\varphi_i}(l)$-th user is given by equation (4.2)

$$y_{\varphi_i}(u_{\varphi_i}(l)) = h_{\varphi_i}(u_{\varphi_i}(l)) x_{\varphi_i} + w_{\varphi_i}(u_{\varphi_i}(l)), \tag{4.2}$$

where, $h_{\varphi_i}(u_{\varphi_i}(l))$ is the channel gain of user $u_{\varphi_i}(l)$. $w_{\varphi_i}(u_{\varphi_i}(l))$ is the noise and ICI of user $u_{\varphi_i}(l)$ at sub-band $\varphi_i$. Maximum ratio combining (MRC) is performed on the signal received $y_{\varphi_i}(u_{\varphi_i}(l))$ by the receiver treating the ICI as white noise as

$$\tilde{y_{\varphi_i}}(u_{\varphi_i}(l)) = \frac{h^H_{\varphi_i}(u_{\varphi_i}(l)) y_{\varphi_i}(u_{\varphi_i}(l))}{||h_{\varphi_i}||}, \tag{4.3}$$

$$= \sqrt{g_{\varphi_i}(u_{\varphi_i}(l))} x_{\varphi_i} + z_{\varphi_i}(u_{\varphi_i}(l)), \tag{4.4}$$

SIC receivers always decode the signal in an ascending order of the channel gain $g_{\varphi_i}(u_{\varphi_i}(l))$ which is normalized by the noise and ICI i.e. $(g_{\varphi_i}(u_{\varphi_i}(l)))/(z_{\varphi_i}(u_{\varphi_i}(l)))$.

Thus the user $u_{\varphi_i}$ can eliminate the interference caused by $j$-th user whose gain is lower than the user's gain. The throughput of user $u_{\varphi_i}(l)$ at sub-band $\varphi_i$ for the scheduled user set $U_{\varphi_i}$ can be represented as (4.5)[22].

where, $g_{\varphi_i}(u_{\varphi_i}(l)) = ||h_{\varphi_i}(u_{\varphi_i}(l))||^2$ is the equivalent channel gain and $z_{\varphi_i}(u_{\varphi_i}(l))$ be the equivalent noise and ICI gain after MRC. The average power of $z_{\varphi_i}(u_{\varphi_i}(l))$ is $n_{\varphi_i}(u_{\varphi_i}(l)) = E[|z_{\varphi_i}(u_{\varphi_i}(l))|^2]$.

$$R_{\varphi_i, U_{\varphi_i}}(u_{\varphi_i}(l))) = B \log_2 \left[ 1 + \frac{g_{\varphi_i}(u_{\varphi_i}(l)) \beta_{\varphi_i}(u_{\varphi_i}(l))}{\sum g_{\varphi_i}(u_{\varphi_i}(l)) \beta_{\varphi_i}(u_{\varphi_i}(j)) + n_{\varphi_i}(u_{\varphi_i}(l))} \right], \tag{4.5}$$

where, $\sum$ refers to $\sum_{j \in U_{\varphi_i}}, \frac{g_{\varphi_i}(u_{\varphi_i}(l))}{n_{\varphi_i}(u_{\varphi_i}(l))} < \frac{g_{\varphi_i}(j)}{n_{\varphi_i}(j)}$.

In the proposed architecture, the whole set of sub-bands of $\varphi$ are accessible in each cell. All CI users are assigned with $\varphi_1$ sub-band in all the cells but not shared with the edge users (FRF=1). The rest of the system bandwidth is arranged in the edge area

in a way to keep the ICI minimum. The proposed 6-sectored MFFR requires lesser splitting of sub-bands than the conventional sectored FFR. The proposed technique divides the bandwidth in $m-2$ sub-bands in contrast to the conventional sectored FFR where total $m$ splitting of sub-bands are required in each cell. Thus the sub-band numbers are reduced in our proposed model whereas all the sub-bands are present in all the cells. Moreover, the splitting of sub-band within a cell enables ICI to reduce noticeably.

### 4.6.2 User Scheduling and Power Allocation

The obtainable throughput of multi-user communication is greatly affected by the resource allocation and user scheduling which are interlinked with each other [10]. The proportional fair (PF) based scheduling and waterfilling algorithm is chosen as the scheduling method and power allocation strategy respectively. PF scheduler balances between user throughput and user fairness. The PF scheduling approach is used in many recent works of NOMA network [10, 22, 72]. PF scheduler focuses on obtaining better throughput by preferring the users with better channel state which, in turn, causes unfairness in scheduling. The waterfilling power allocation is applied based on the channel condition. Transmission power for $k^{th}$ user in sub-band $\varphi_i$ can be expressed by (4.6) as

$$p_{\varphi_i}(k) = \frac{P}{\sum_{j \in U_{\varphi_i}} \left(g_{\varphi_i}(j)/n_{\varphi_i}(j)\right)^{-\alpha_{FPA}}} \left(\frac{g_{\varphi_i}(k)}{n_{\varphi_i}(k)}\right)^{-\alpha_{FPA}} \tag{4.6}$$

where, $\alpha_{FPA}$ is the decaying factor. This fractional allocated power equation can be converged into equal power allocation in all users if $\alpha_{FPA} = 0$. As $\alpha_{FPA}$ increases, higher power level is assigned to the user with lower $g_{\varphi_i}(k)/n_{\varphi_i}(k)$ value i.e. the users with poorer channel condition.

The sum-rate is maximized basing on the following transmission power constraint

$$\max \sum_k R_k \tag{4.7}$$

$$s.t. \sum_k P_k \leq P.$$

**Algorithm 1** pseudo-code of frequency and power allocation procedure

Step:1 Initialization: user number per cell $K$, number of obtainable sub-bands in each cell $m$, set of sub-bands in each cell $\varphi$ and number of the scheduled users in user set $U_{\varphi_i}$ is $L$ in sub-band $\varphi_i$.

Step:2 Divide the total sub-bandwidth of a cell $\varphi$ into $\varphi_{CE}$ and $\varphi_{CI}$ for CE and CI users respectively.

Step:3 Set the distance $d_{CI}$ for CI user selection.

Step:4 $d_{CE}$ = Cell Radius - $d_{CI}$

Step:5 **for** a user $u_{\varphi_i}(l)$ in user set $U_{\varphi_i}$
**if** $d_l \leq d_{CI}$
assign sub-band from $\varphi_{CI}$
**else**
assign sub-band from $\varphi_{CE}$
**end**

Step:6 Allocate power by multi-level waterfilling algorithm to every user $u_{\varphi_i}(l)$ in user set $U_{\varphi_i}$
considering the total power constrain.

Step:7 Users are scheduled by PF metric.

Step:8 **if** all sub-bands have been assigned
final power allocation
**else**
repeat from step 5 to assign a new sub-band to a user.
**end**

## 4.7 Conclusion

Frequency reuse is an important tool to keep the ICI minimum. This chapter explained the benefits of using frequency reuse, discussed various type of reuse techniques and compared among them. FFR keeps the ICI less than SFR but with compromised bandwidth efficiency. It also acts as trade-off between overall performance enhancement and the throughput improvement of the edge users. SFR is highly bandwidth efficient but SFR with NOMA may face performance degradation due to the unfairness caused by the user pairing. Moreover, the ICI in SFR is much high. Sectored FFR combines the advantages of FFR and SFR. A new modified sectored FFR is proposed for NOMA Multi-cellular Networks. Cells are sectored into cell interior and edge, and then the exterior part of the cell is further divided into 6-sector with

a lesser splitting of the sub-band set than the conventional one. This lesser splitting will enable the accumulation of more users in each cell which enhances the network capacity and facilitates user grouping. Also, the bandwidth sectorization results into the reduction of the effect of inter-cell interference. We adopted proportional fairness approach for allocating sub-band and power. It is observed that our proposed modified 6-sectored FFR generates less ICI, saves radio resources and thereby achieves much higher sum rate than SFR and No-FFR. We will compile this IM technique along with the beamforming technique mentioned in chapter 3 in the next chapter.

# CHAPTER 5

# mmWave-MIMO NOMA NETWORK

## 5.1 Introduction

The interference mitigation technique mentioned in chapter 4 is implemented in the mmWave-MIMO NOMA system model mentioned in chapter 3. A user scheduling is proposed based on the real-time non-real time traffic class and data rate requirement and also a multi-level water-filling power allocation algorithm is proposed.

## 5.2 Complete System Model

The proposed mmWave-MIMO system model has one BS equipped with $N_t$ antennas and $N_t^{RF}$ number of RF chains such that, $N_t >> N_t^{RF}$. The $N_S$ data streams are being transmitted from the antenna array of the BS to users each with $N_r$ antennas ($N_r = N_t$) and $N_r^{RF}$ RF chains. Proposed model is illustrated in Fig. 5.1. In the transmitter section, there are main three subsystems: digital precoder, RF chain and fuzzy based analog precoder. The base band signal is processed by $N_t^{RF} \times N_S$ dimensional digital precoder, then converted into $N_S \times N_t^{RF}$ dimensional RF signal using RF chain. The RF chains are selected as per the requirements of each sector of the cell. Then the RF chains are coded with fuzzy based analog precoder. The output of the RF chain is fed into PSs for generating N parallel signals with same amplitude $1/\sqrt{N}$ and different phases. Finally, the signal with required phase will be fed into Fuzzy based switching matrix for transmitting with MIMO antenna array.

To overcome the interference, all the sub-carriers are not assigned to be transmitted in all directions. A frequency allocator allocates the sub-carrier basing on the user location within a cell. The sub-carriers are selected as per the sub-bands distribution shown in fig. 4.4 which is discussed in section of chapter 4.

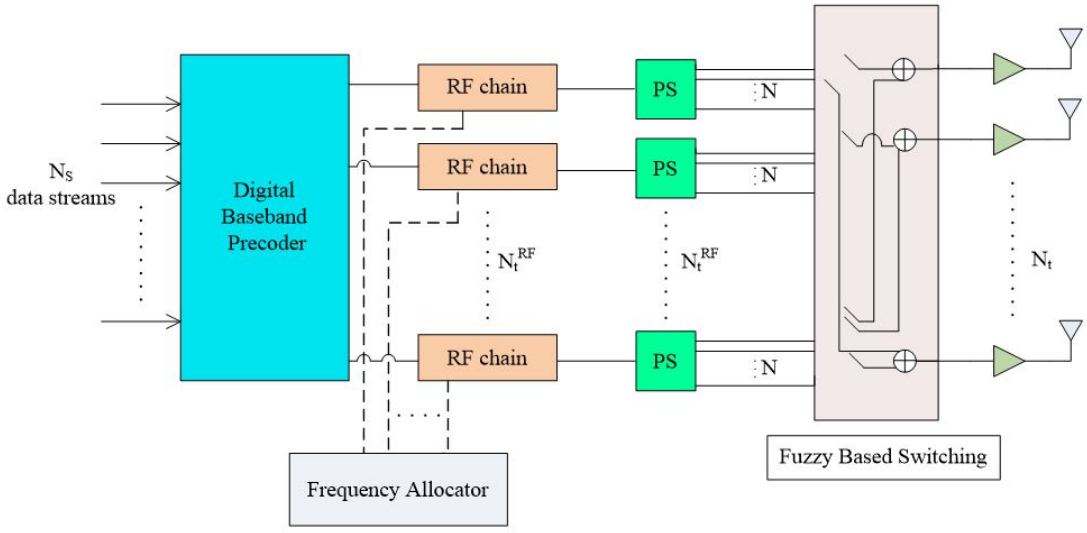


**Fig. 5.1.** Proposed complete system model.

The transmitted signal can be expressed as

$$x = \mathbf{F}s \tag{5.1}$$

where, the hybrid precoding matrix $\mathbf{F} = \mathbf{F}_{AB}\mathbf{F}_{DB}$ is applied to transmitted symbol vector $s = \begin{pmatrix} s_1 & s_2 & \dots & s_{N_S} \end{pmatrix}^T \epsilon \, \mathcal{C}^{N_s \times 1}$ in the baseband with $\mathbb{E}\left[ss^H\right] = I_{N_s}$. $\mathbf{F}_{DB}$ be an $N_t^{RF} \times N_t$ baseband digital precoder matrix. For FC structure where the data streams are connected to all RF chains, $\mathbf{F}_{DB}$ is expressed as

$$\mathbf{F}_{DB} = \begin{pmatrix} d_{11} & \cdots & d_{1N_s} \\ \vdots & \ddots & \vdots \\ d_{N_t^{RF}1} & \cdots & d_{N_t^{RF}N_s} \end{pmatrix} \tag{5.2}$$

But we consider the SC structure where single RF chain is connected to each data stream. This reduces $\mathbf{F}_{DB}$ to a diagonal matrix $\mathbf{F}_{DB} = diag\left(d_{11}, d_{22}, \dots, d_{N_t^{RF}N_s}\right)$. The digital precoded data is directly fed into the analog beamformer of the corresponding sub-array. $\mathbf{F}_{AB}$ be the $N_S \times N_t^{RF}$ analog beamforming matrix which can be expressed as

$$\mathbf{F}_{AB} = \begin{pmatrix} a_1 & 0 & \dots & 0 \\ 0 & a_2 & \dots & 0 \\ \vdots & \vdots & \ddots & \vdots \\ 0 & 0 & \dots & a_{N_t^{RF}} \end{pmatrix} \tag{5.3}$$

We consider the frequency-flat channel for narrowband frequency. Assuming the widely accepted Saleh-Valenzuela channel model for L number of paths, the channel matrix $\mathbf{H}\ \epsilon\ \mathcal{C}^{N_r \times N_t}$ can be expressed as

$$\mathbf{H} = \gamma \sum_{l=1}^{L} \alpha_l \mathbf{a}_r(\phi_l^r)\mathbf{a}_t^H(\phi_l^t) \tag{5.4}$$

where $\alpha_l$ is the complex gain for $l^{th}$ path with $\mathbb{E}\left[|\alpha_l|^2\right] = 1 = 1$ and $\gamma$ is a normalization factor. $\phi_l^r \epsilon\, [0, 2\pi]$ and $\phi_l^t \epsilon\, [0, 2\pi]$ are the $l^{th}$ paths angle of departure (AOD) and angle of arrival (AOA) respectively. $\mathbf{a}_r(\phi_l^r)$ and $\mathbf{a}_t^H(\phi_l^t))$ be the array response vectors of BS and user respectively. Considering uniform linear array (ULA), $\mathbf{a}_t(\phi_l^t))$ can be expressed as

$$\mathbf{a}_t(\phi_l^t) = \frac{1}{\sqrt{N_t}} \left[1, e^{j\frac{2\pi}{\lambda} d \sin\phi_l^t}, \dots, e^{j(N_t-1)\frac{2\pi}{\lambda} d \sin\phi_l^t}\right] \tag{5.5}$$

Then the received signal will be

$$\mathbf{r} = \sqrt{\beta}\mathbf{H}\mathbf{F}\mathbf{s} + \mathbf{n} \tag{5.6}$$

where $\beta$ be the power coefficient and $\mathbf{n}\ \epsilon\ \mathcal{CN}(0, \sigma^2)$ be the AWGN vector. The user combines the received signal via a hybrid combiner $\mathbf{W} = \mathbf{W}_{AB}\mathbf{W}_{DB}$ where $\mathbf{W}_{AB}$ be the analog RF combiner and $\mathbf{W}_{DB}$ is the digital combiner. So, the received signal after processing is

$$\mathbf{y} = \sqrt{\beta}\mathbf{W}^*\mathbf{H}\mathbf{F}\mathbf{s} + \mathbf{W}^*\mathbf{n} \tag{5.7}$$

### 5.2.1 Switching algorithm

In our FeE-HBS system, the signal with required phase will be fed into Fuzzy based switching matrix for transmitting with MIMO antenna array. This switching is designed which aims to maximize the sum rate. The performance of precoder and switching matrix system depends on selection of appropriate PSs. However,

optimal search algorithm increases the complexity of the HBS. The fuzzy based low complexity design requires to compromise with the performance of the HBS. In this work, we have considered that the CSI information are available at the receiver as per these estimation techniques. In addition, AoD of a group of uses takes values from $[0, 2\pi]$ whereas the mean AoA of a group follows uniform distribution over $\pi/3$ sector. Fig. 3.7 shows fuzzy logic controller (FLC) for the switching matrix operation. Based on the fuzzy inference rules, FLC may select PS to be switched on considering differentiation of AoA, AoD, data rate demand. Each variable contains three linguistic terms low (L), medium (M) and High (H) and they follow gaussian membership function. The relation between the input and output membership functions was shown in fig. 3.7 in chapter 3.

## 5.3 User Scheduling and Power Allocation in NOMA Network

The obtainable throughput of multi-user communication is greatly affected by the power allocation and user scheduling which are interlinked with each other [10]. Most previous works study the scheduling method without considering the users' connectivity criteria and traffic class which becomes unrealistic in the real communication scenario. Different types of users (e.g. real time (RT) and non-real time (nRT), user with lower data rate requirement (audio data) and user with higher rate requirement (video data) etc.) are served in the network. So, in our work, we considered these parameters for picturizing a realistic communication environment. In case of traffic class metric, we preferred RT traffic over nRT traffic for frequency allocation. Initially, we scheduled the users basing on their traffic class i.e. RT and nRT users. The users are served on a first-come first-serve basis i.e. the RT users are served sub-bands with priority than nRT users. Thus, the QoS of RT users are facilitated [67]. In addition, the data rate requirement of users is also considered. Unlike the users with low data rate requirement, the users with high rate requirement are assigned an additional sub-band from the unused spectrum along with its assigned frequency band. Users which require low data rate are assigned the regular sub-bands based on its traffic class. These facilitates the practical communication scenario extensively.

The multi-level waterfilling algorithm is chosen to be the power allocation strategy. The power allocation is achieved basing on two parameters i.e. the channel conditions and the distance of the UE from the BS. In this work, we focus on enhancing the overall throughput i.e. the system is proportional fair. So we allocate more power to

the user with better channel condition and less power to the worse channel user. Also the user close to the BS are served better power than the users far away from the BS. We chose multi-waterline levels for channels basing on their maximum transmission power requirement. The optimal allocation scheme delivers a better throughput at the cost of increased computational complexity. Therefore, a suboptimal approach is adopted which provides a trade-off between the system throughput and complexity of the system. The fractional power allocation (FPA) is used as the suboptimal method which is inspired from the uplink power control in LTE network [22]. FPA is very simple to implement. It is used to adjust the transmit power allocation dynamically to the users of a sub-band according to the channel gain and it enables a fractional power count basing on the sorted channel gain [87] to user k at sub-band $\varphi$.

The sum-rate is maximized basing on the following transmission power constraint

$$\max \sum_{k} R_k \tag{5.8}$$

$$s.t. \sum_{k} P_k \leq P.$$

Also

$$\sum_{i} \varphi_i \leq \varphi.$$

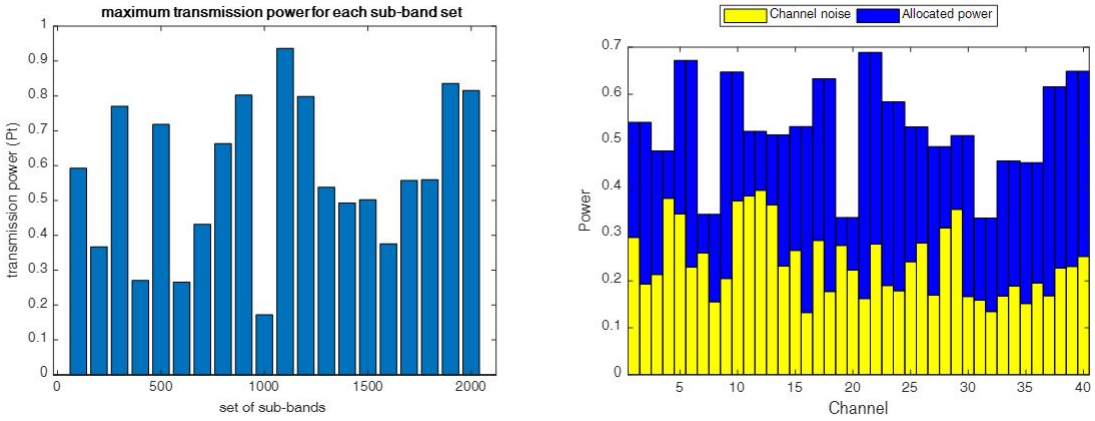


**Fig. 5.2.** Transmit power and multi-level waterfilling power allocation to different sub-bands.

Fig 5.2 shows us the different transmit power level of different sub-bands. We divide the total bandwidth into 20 set of sub-bands. These set of sub-bands are assigned with multi power level in order to apply multi-waterfilling algorithm. The

**Algorithm 2** Algorithm for sub-carrier and power allocation

Step:1 divide total bandwidth $\phi$ into a set of sub-bands and assign to frequency array.

Step:2 i = 1;
j = 1;

Step:3 **for** i = 1 : user number
**if** u(i) == RT users
**if** data rate of u(i) $R(i) \geq R_{th}$
frequency distr matrix1(i) = frequency array(j) + additional unused band;
**else**
frequency distr matrix1(i) = frequency array(j);
**end**
j = j + 1;
**else**
**end**
i = i + 1;
**end**

Step:4 **for** i = 1 : user number
**if** u(i) == nRT users
**if** data rate of u(i) $R(i) \geq R_{th}$
frequency distr matrix1(i) = frequency array(j) + additional unused band;
**else**
frequency distr matrix1(i) = frequency array(j);
**end**
j = j + 1;
**else**
**end**
i = i + 1;
**end**

Step:5 **Adopting waterfilling as power allocation algorithm**

Step:6 **for** i = 1 : number of sub-band set
power allocation will be a function of channel condition and distance
multi-level waterfilling is adopted as the power allocation
**end**

reason of choosing multi-level waterfilling as the power allocation strategy is that, all the channels do not require equal power level to transmit the data. Thus, the power level to any sub-band is assigned as per the requirement of the channel.

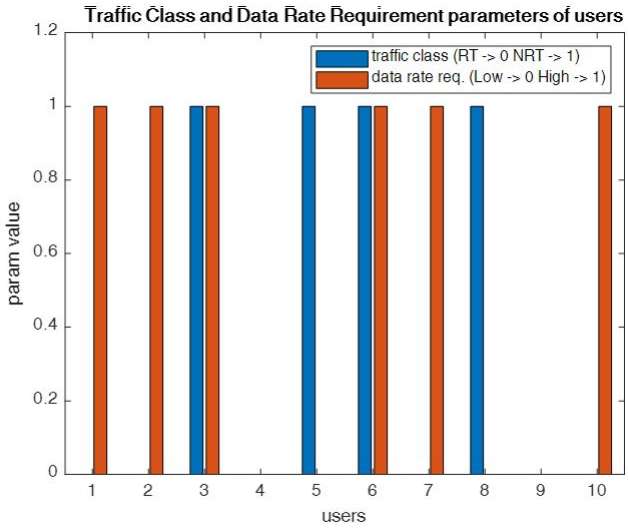


**Fig. 5.3.** User parameters representation.

Fig 5.3 shows the visual representation of different types of users. For this example of 10 users, six users are considered as RT users and four users (blue marked) are considered nRT users. The users based on data rate requirement are also displayed. Here, four users are of low data requirement and six users are required with high data rate.

We considered a 10-user scenario where the users are categorized based on their traffic class. The sub-band allocation is achieved based on their traffic class as we can see from fig 5.4. The RT users are assigned with sub-bands before the nRT users. It can be observed that user 1,4,5, 8 and 10 are the RT users where the user 2,3,6,7 and 9 are the nRT users. Thus the RT user 1, 4, 5, 8 and 10 are assigned with the sub-band at first and then the nRT user 2,3,6,7 and 9 are served with the sub-bands gradually.

After allocating the sub-band as per the traffic class, we also prioritize the users with high data rate requirements over the users with low data rate requirements. As we can see from fig 5.5, user 3, 4, 6, 8 and 10 are the users required with high data rate. These users are allotted with some extra sub-bands in addition to their previously assigned sub-bands. Rest users allotted sub-bands are kept unchanged as the previously assigned sub-bands based on traffic class.

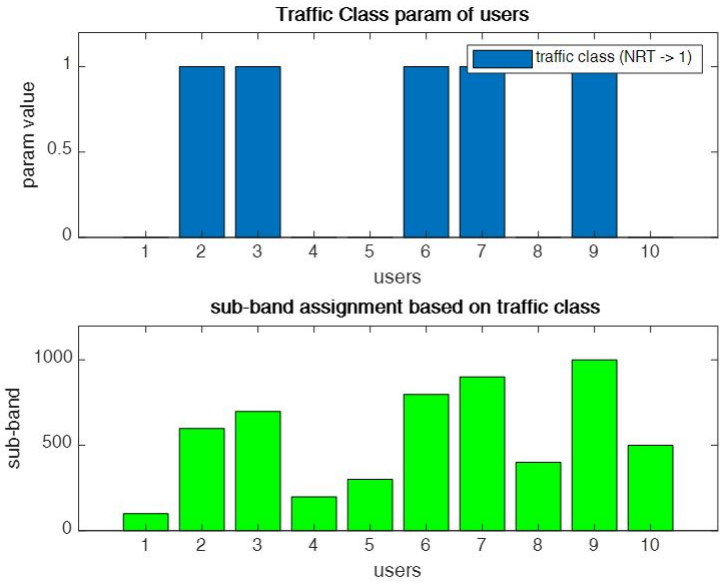


**Fig. 5.4.** Sub-band assignment based on traffic class.

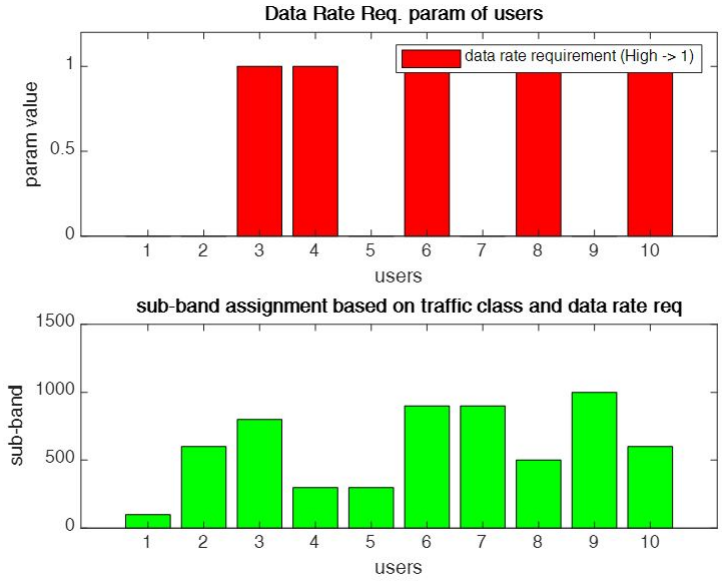


**Fig. 5.5.** Sub-band allocation basing on data rate requirement.

# CHAPTER 6

# RESULTS AND DISCUSSIONS

## 6.1 Introduction

The simulation works of the proposed system model mentioned in chapter 3 and 4 will be discussed in this chapter. The requirements of 5G cellular network like bulk connectivity i.e. enhancing spectral efficiency, obtaining an energy efficient network, reducing latency i.e. increasing the rates, enabling an interference mitigated network etc. were always kept in mind while designing the system model. This chapter shows the effect of the proposed technique on the behavior of the most important evaluation metrics like energy efficiency, data rate, signal-to-noise-plus-interference ratio (SNIR), sum rate etc and compared with the conventional ones.

## 6.2 Evaluation Metrics with Proposed Hybrid Beamforming

In this section, the performance of the proposed network mentioned in chapter 3 is evaluated and compared to the conventional fully connected and sub-connected system. To be more specific, the change in energy efficiency performance with the change in SNIR and in terms of the number of RF chain is showed. Also, the behavior of data rate is monitored while changing the SNIR value for different beamformers. The channel paths are assumed $L = 5$. This work considered $N_t = N_r = 64$ i.e. a large number of transmit and receive antennas are assumed in order to implement the concept of massive MIMO. A frequency-flat channel with perfect CSI is considered.

### 6.2.1 Effect on the energy efficiency behavior for different beamforming

Energy efficiency was a major concern in this work. It is the ratio of SE to the total power consumed at the transmitter. Energy consumption is a disadvantage of using the massive MIMO techniques since large number of RF chains are used. Thus, to achieve a moderate EE is a big challenge which largely varies for different beamforming technique. Fig. 6.1 shows the EE behavior with the change of SNIR considering $N_t^{RF} = N_r^{RF} = N_s = 6$ and $N_t = N_r = 64$ for the system model shown in fig. 3.6. It is observed that, the EE is increased in the sub-connected architecture with the increase of phase shifters per sub-array. Fig. 6.1 shows the increase in the EE for the number of phase shifters, $N = 2, 4$ and 8. It is because the sub-connected structure is independent of PSs. The increase in SE with almost the same energy consumption at the transmitter leads to increase the EE. However, the EE also increases with SNIR value. It is observed that, the proposed fuzzy-based HBS scheme with $N = 8$ outperforms all the conventional sub-connected structures in terms of energy efficiency.

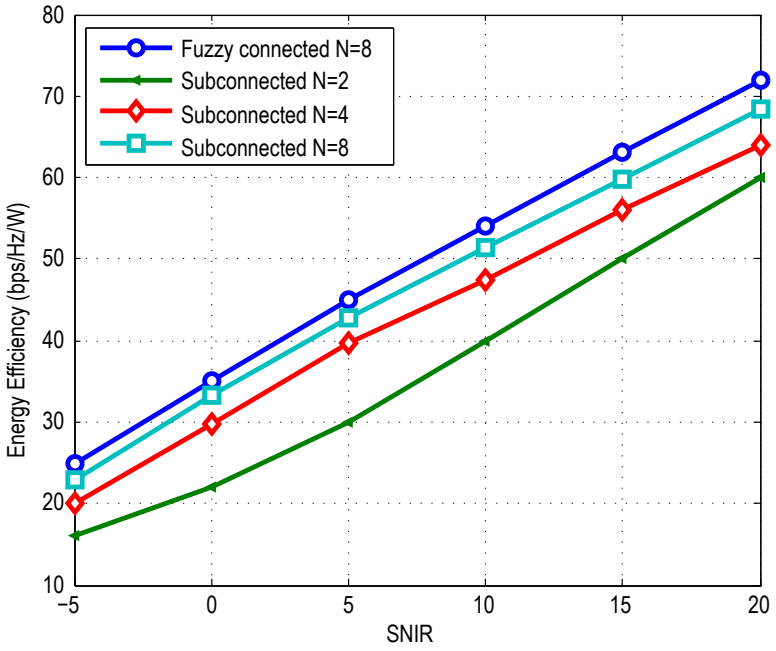


**Fig. 6.1.** Comparison of EE over SNIR of the network considering $N_t^{RF} = N_r^{RF} = N_s = 6$ and $N_t = N_r = 64$.

### 6.2.2 Effect on data rate behavior for different beamforming

The data rates of the all the structures are analyzed in fig. 6.2 for the change in SNR. Both the BS and users are assumed to own perfect CSI. It is observed that, the analog beamforming structure scheme [76] obtains the lowest rate for the same SNR requirement among all connections. Both the digital beamforming structure [76] and the proposed scheme achieves nearly same data rates for any SNR value and outperforms all other structures. But the energy consumption of digital beamforming technique is much higher than the proposed technique. Thus, the Fe-HBS beamforming technique achieves higher data rate with better energy efficiency than any other technique. However, the increase of the number of PSs ($N = 4$) surely allows all the structures to achieve an improved data rate.

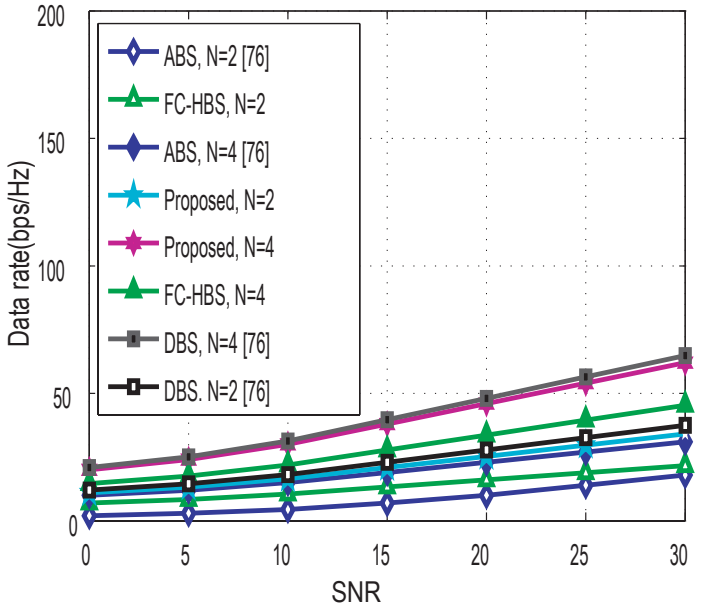


**Fig. 6.2.** The effect of SNR in dB on average data rate in b/s/Hz for N=2 and N=4.

### 6.2.3 Effect on energy efficiency for the change in RF chain

In fig. 6.3, the change in energy efficiency is observed with the change in RF chains. It is noticeable that, the energy efficiency of the digital beamformer lags much behind than that of the proposed FeE-HBS system. The proposed sub-connected HBS outperforms the digital structure in terms of EE specially when $N_t^{RF}$ is low. Nonetheless, as the number of $N_t^{RF}$ is increased, the energy efficiency of the system

increases but becomes nearly saturated at higher $N_t^{RF}$. This is because the number of PSs is independent of number of $N_t^{RF}$ in sub-connected architecture. So the energy consumption remains almost constant for the change in the range of RF chains. But since the SE increases with the increase of $N_t^{RF}$, the overall system becomes energy efficient for the enhanced SE with nearly constant energy consumption. However, for a large number of RF chain, energy consumption gets increased which results in a reduction in EE.

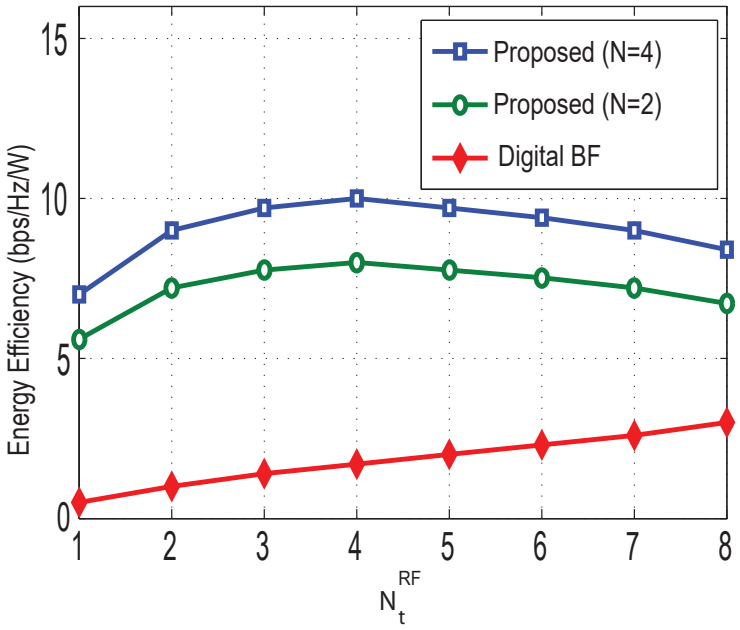


**Fig. 6.3.** The effect of $N_t^{RF}$ on energy efficiency for proposed HBS and digital beamforming structure for N=2 and N=4.

## 6.3 Evaluation Metrics with Proposed Frequency Reuse Technique

To evaluate the performance of the proposed FFR technique mentioned in chapter 4 with NOMA, this section presents numerical results for the percentage of total allocation of sub-bands and SNIR as a function of cell radius; and sum rate as a function of SNIR and is compared with the other techniques i.e. SFR and no FFR. The SFR technique is adopted from Abdullahi et al.'s SFR technique in OFDM domain in [55] and then applied it for NOMA network. The simulation parameters used here are shown in the table 6.1. MATLAB R2016a is used for the simulation.

**Table 6.1:** Simulation Parameters for Implementing the Frequency Reuse Techniques

| Parameters | Value |
|---|---|
| inter-site distance (m) | 500 |
| frequency resource blocks, N | 2 |
| transmit antenna gain (dBi) | 14 |
| transmission power (dBm) | 23 |
| number of antenna at UE | 1 |
| the receiver antenna gain (dBi) | 0 |
| shadowing standard deviation (dB) | 8 |
| receiver sensitivity (dBm/Hz) | -174 |
| sub band bandwidth (kHz) | 150 |
| overall transmission bandwidth (MHz) | 10 |

### 6.3.1 Effect of the proposed technique on number of sub-bands

Fig. 6.4 shows the percentage of total allocated sub-bands for no FFR, SFR and the proposed modified sectored FFR (MFFR) for the normalized distance between the BS and UE. The aim is to reduce the splitting of the total bandwidth allotted per cell by implementing the proposed scheme. It can be noticed that, the proposed MFFR scheme issues the lowest allocation of sub bands for a particular cell radius. That is, we can save some sub-bands in the proposed scheme. This lower splitting can incorporate large number of devices in each sector of a cell than the conventional sectored FFR. However, the allocation in sub-bands increases with the increase of cell radius but still lower than SFR and no FFR. Percentage allocation is always one irrespective of cell radius in case of no FFR since all the sub-bands can be used by all the users within a cell.

### 6.3.2 Effect of the proposed technique on SNIR

Improving the SNIR to enhance the overall capacity of the system was a prime focus of this work. Fig. 6.5 indicates the SNIR behavior with the increase in the distance between BS and user. SNIR improvement are surely to be achieved in all frequency reuse techniques since ICI is mitigated to a great extent. It can be seen from the figure that the SNIR decreases as the distance of UE from BS increases. However, the SNIR of the proposed method in NOMA network is far-reaching from the SFR [55] in NOMA and no FFR technique for a fixed cell radius. It is due to the fact that, the proposed modified sectored FFR ensures the minimum amount of interference by dividing each cell into sectors and assigning them unique sub-bands

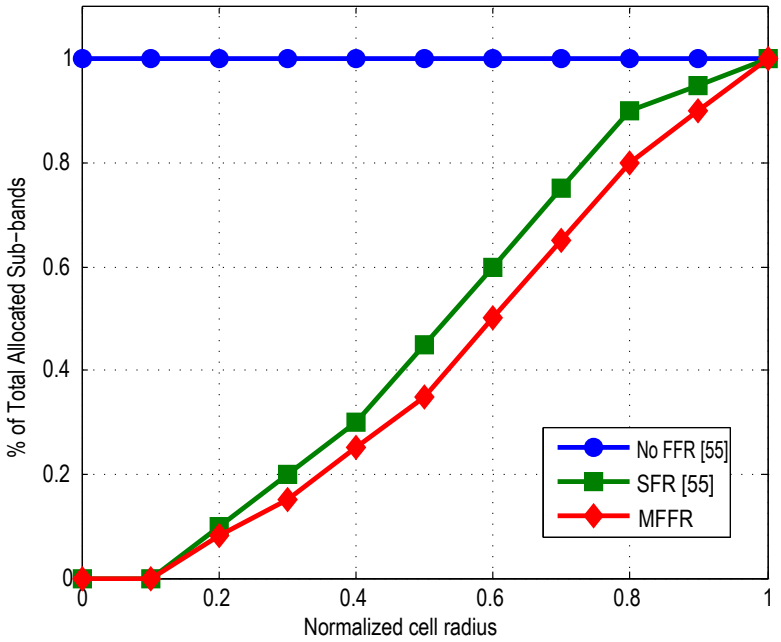


**Fig. 6.4.** Percentage of allocated sub-bands as a function of normalized cell radius for no FFR, SFR and proposed FFR algorithms. Proposed MFFR ensures lowest allocation of sub-bands.

such a way that they do not interfere with each other. This increases the SNIR of each user, specially of the edge users. The SNIR for the system without any frequency reuse or no FFR scheme falls much behind than SFR and proposed MFFR. It is due to the presence of large amount of inter-cell interference in each cell caused by the neighboring cells. SFR has lower amount of SNIR than the proposed scheme for the same distance from the BS because of the presence of higher ICI in each cell than the proposed scheme. This ICI occurs from engaging the interior sub-bands of one cell in the exterior area of another cell.

### 6.3.3 Effect of SNIR on sum rate

Fig. 6.6 shows the effect of SNIR on the sum rate for different fractional frequency reuse techniques. The sum rate increases with the improvement of signal quality noticeably irrespective of which frequency reuse technique is used. MFFR with fair and proportional scheduling outperforms all other techniques in terms of sum rate. This is because the proposed FFR method ensures lower portion of interference along with the availability of all sub-bands in all cells with much lesser splitting unlike the other conventional methods. Moreover, the MFFR with proportional scheduling

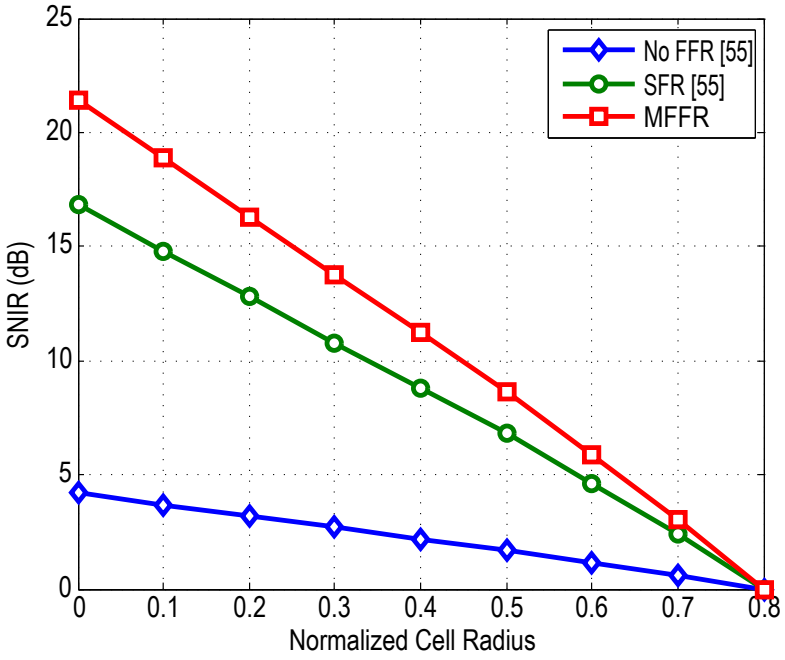


**Fig. 6.5.** SNIR as a function of cell radius. The proposed algorithm outperforms SFR and no FFR in terms of signal quality.

achieves much higher sum rate than the one with fair scheduling. In the fair method, a fair allocation to users is ensured i.e. the weak users were given priority over the strong user in sub-band allocation. It enhances the performance of the weak users noticeably, but the overall network performance is compromised. The proportional MFFR focused on the improvement of overall system performance, rather than of any distinct user.

By serving the strong user over the weaker one, modified FFR with proportional scheduling method outperforms all the other techniques in terms of sum rate. Sum rate for the no FFR scheme lags behind due to the huge interference not mitigated in each cell.

## 6.4 Effect on Sum Rate for the Complete System Model

Fig. 6.7 shows the behavior of sum rate for the complete system model mentioned in chapter 5. The fuzzy based beamforming technique proposed in chapter 3 and the interference mitigation technique mentioned in chapter 4 are compiled in chapter 5. Then the complete model is verified in comparison to the FFR model demonstrated in [56]. It can be observed that, the performance of the FLC based hybrid beamforming

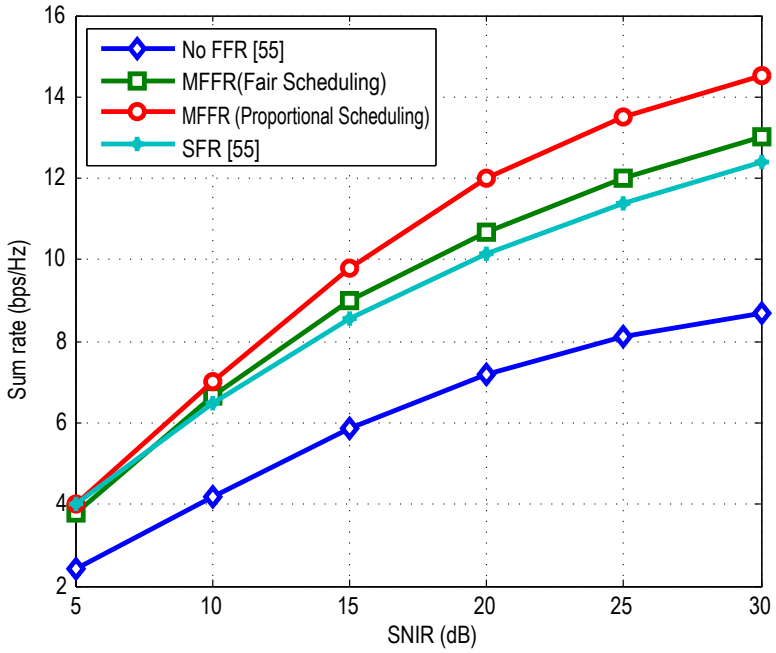


**Fig. 6.6.** Sum rate as a function of SNIR. The proposed algorithm outperforms SFR and no FFR in terms of sum rate.

is enhanced than the one without FLC for both proportional NOMA and fair NOMA because the proposed switching based beamforming method can produce higher SE at larger number of RF chain also with almost constant energy consumption. Thus it produces better sum rate for same target SNIR than the one without FLC. The sum rate increases at higher SNR value for all the methods. It can also be noticed that, the proportional resource allocation produces far better output than the fair scheduler. It is because the proportional fair NOMA focuses on improving the overall network throughput unlike fair NOMA i.e. focusing on cell edge users' performance.

## 6.5 Comparison of the Proposed Fuzzy-FFR based MIMO-NOMA, MIMO-NOMA and MIMO-OMA

The proposed fuzzy-FFR based MIMO NOMA model is compared with the existing MIMO-OMA model and the popular Zeng et al.'s MIMO-NOMA model mentioned in [1]. Fig. 6.9 and fig. 6.10 show that the proposed method outperform Zeng et al.'s MIMO-NOMA and MIMO-OMA.

Fig. 6.8 shows the sum rate performance of MIMO-NOMA and MIMO-OMA for two-users and three-users scenario. The sum rate improves for both cases of

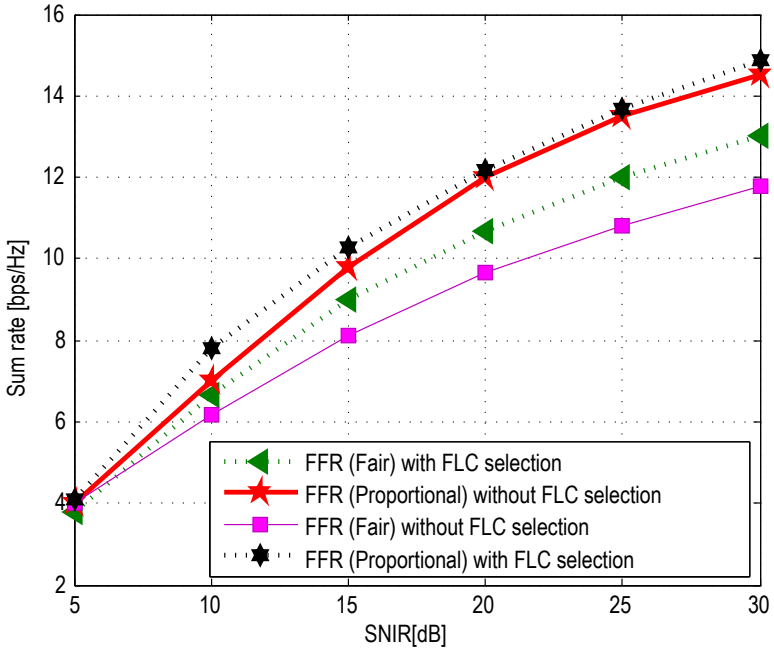


**Fig. 6.7.** Sum rate as a function of SNIR. The proposed FFR technique along with the FLC based beamforming with proportional fairness algorithm outperforms other techniques in terms of sum rate.

MIMO-NOMA and MIMO-OMA with the increase in power coefficient value of user 1. It is because higher power is alloted to the users with better channel condition. MIMO-OMA lags much behind both the proposed and Zeng et al.'s MIMO-NOMA cases. The proposed NOMA technique certainly generates higher sum rate value than Zeng et al.'s NOMA for a particular power coefficient of user 1. Changing the user number causes a decrease in performance of all the MIMO-NOMA and MIMO-OMA techniques because sum rate gets lower when more number of users are present in the cluster resulting into more interference. Nonetheless, the proposed method improves the network performance greatly for 3-user case than in MIMO-NOMA [1] because a lower interference environment is provided in the proposed work which, in turn, does not let to reduce the sum rate drastically.

Fig. 6.9 shows the effect of SNIR on sum rate for different values of the distance between the BS and users. Fig. 6.9 exhibits some fluctuations, but it can be clearly seen that the sum rate of both the MIMO-NOMA techniques and the MIMO-OMA technique gradually increase with the increase in SNR. Both the NOMA techniques produce better sum rate than the OMA technique. The proposed scheme exhibits better sum rate than Zeng et al.'s NOMA technique in [1] for low to normal range of

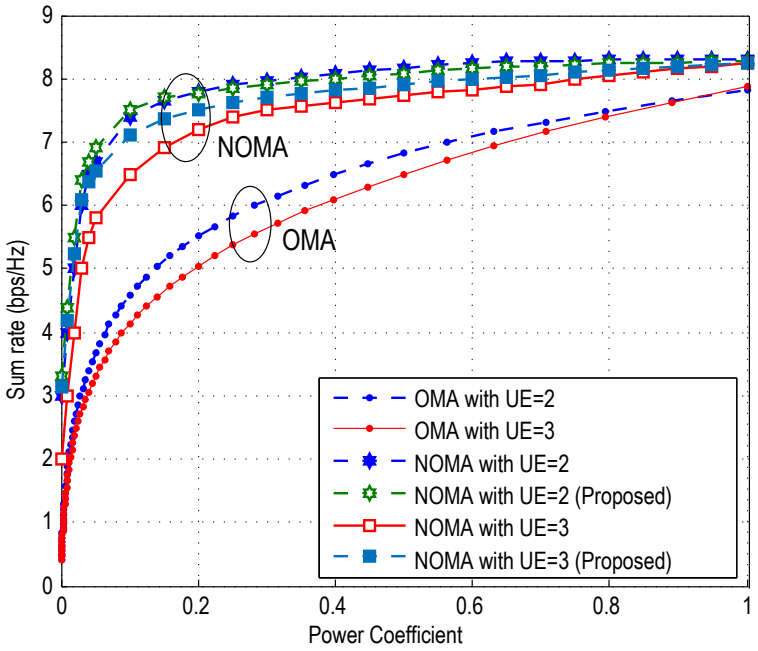


**Fig. 6.8.** Sum rate for proposed MIMO-NOMA, existing MIMO-NOMA [1] and MIMO-OMA as a function of power coefficient.

SNR. At high SNR, it is approximately same as MIMO-NOMA [1].

The system is also evaluated for unequal distance from BS to different users. It can be observed that, NOMA achieves higher sum rate than OMA for asymmetric distances and this performance gap increases with the SNR. Also, for the two cases that have been mentioned here i.e. normalized distance of 0.5 and 1 and normalized distance of 0.75 and 1, NOMA creates larger performance gap with OMA as the discrepancies in distance of the users from the BS increases. This indicates that the benefit of MIMO-NOMA can be achieved than MIMO-OMA with large performance gap if user pairing is done between the users with higher discrepancies in distance.

Fig. 6.10 also demonstrates the performance of sum rate with the change in SNIR for different number of transmit and receive antennas. For both the cases of $N_t = N_r = 4$ and $N_t = N_r = 8$, the sum rate of the proposed MIMO-NOMA is greater than the Zeng et al.'s MIMO-NOMA for low to normal range of SNIR. However, when the number of transmit and receive antennas are increased, the sum rate performance improves largely. This result depicts that capacity is largely improved when large number of antenna elements are included i.e. MIMO evolves into massive MIMO. The performance of the proposed system slightly declines at higher SNIR value. But the performance is higher than the MIMO-NOMA mentioned in [1] from low to normal

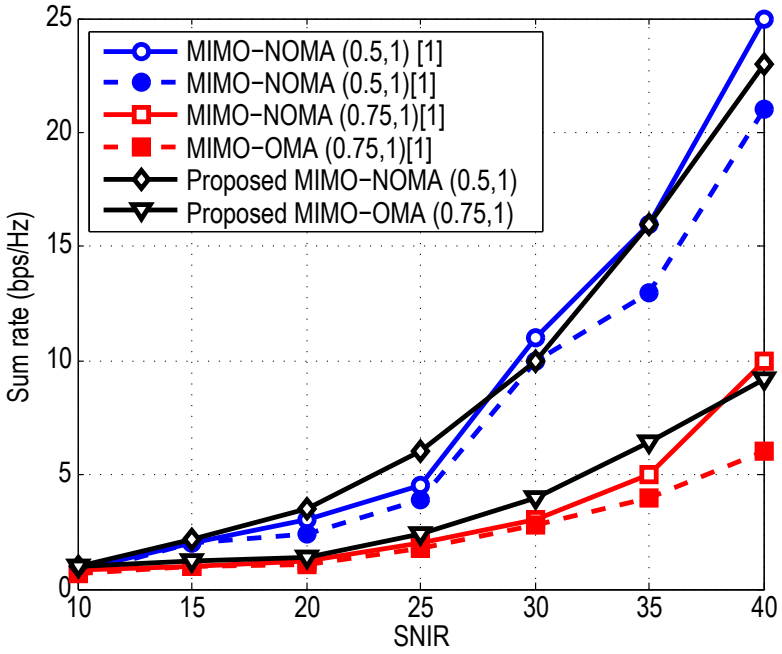


**Fig. 6.9.** Sum rate for proposed MIMO-NOMA, existing MIMO-NOMA [1] and MIMO-OMA as a function of SNR for different distances between BS and users.

range of SNIR for both the 4X4 and 8X8 cases.

## 6.6 Conclusion

This chapter shows the behavior of some important user parameters for the implementation of proposed beamforming technique and frequency reuse technique. Article 6.2 displays the change in energy efficiency for SNIR and data rate with the change in SNR for analog, digital and the proposed beamforming technique which is briefly discussed in chapter 3. The energy efficiency with the change in the number of RF chain is also observed. Comparing all the parameters, it can be decided that the proposed FeE-HBS turns out to be the most energy efficient with enhanced spectral efficiency. The chapter also compared the performances of different frequency reuse technique i.e. strict FFR, SFR and sectored FFR discussed in chapter 4. The performance of the novel sectored FFR proposed in chapter 4 is evaluated in this chapter and it is observed that the proposed technique achieves higher sum-rate than all other conventional techniques by making the ICI less while maintaining lesser splitting of sub-bands. Finally, the evaluation metric for the complete system model combining the beamforming technique and frequency reuse technique depicts the performance of

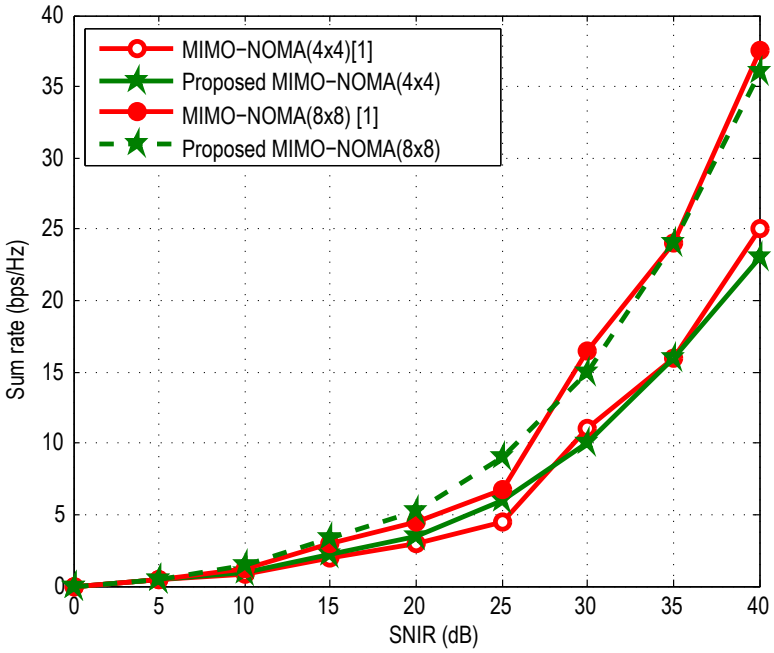


**Fig. 6.10.** Sum rate for proposed MIMO-NOMA, existing MIMO-NOMA [1] and MIMO-OMA as a function of SNIR for different $N_t$ and $N_r$

the design and shows that the proposed model is capable of outperforming all other techniques in terms of sum rate. The performance is evaluated for different resource allocation also i.e. fair and proportional scheduling. The proportional scheduling focuses on providing better overall capacity than the fair scheduler. The proposed model is also compared with existing MIMO-NOMA and MIMO-OMA models in terms of sum rate for multiple users with asymmetric distances. MIMO-NOMA outsmarts MIMO-OMA in all aspects. The proposed MIMO-NOMA model increases the performance gap with MIMO-NOMA than the existing MIMO-NOMA when the discrepancies in distance and user number per cluster are increased i.e. more practical communication scenario. It is observed that the proposed model in this thesis is capable of outperforming other work even considering more practical communication scenario.

# CHAPTER 7

# CONCLUSION AND FUTURE WORK

## 7.1 Conclusion

This thesis work provides a comprehensive Introduction of the promising 5G technologies and focuses on the incorporation of these exciting features to build an efficient and time-demanding 5G network. NOMA is been chosen as the multiple access technique over any OMA technologies in this work. NOMA can overcome the limitations of OMA based networks that does not permit frequency reuse within a cell. It eliminates the connectivity restriction of users imposed by OFDMA, ensures less latency and enhances the SE compared to all other OMA technologies. A power domain downlink NOMA with superposition coding and SIC receiver is studied. The research results have showed NOMA to be a better option in terms of many important parameters i.e. sum rate, SINR, SE etc. The work also discusses how NOMA adopts other 5G technologies like MIMO, beamforming and mmWave communication. The NOMA network is incorporated with mmWave transmission in this research work. The use of the large unutilized spectrum validates more IoT devices inside the family of bulk user nodes enabled by NOMA network. The high frequency spectrum of mmWave transmission lowers the latency enormously. But due to the path loss suffered by mmWave, beamforming with MIMO is assimilated with mmWave-NOMA network. Several beamforming techniques are studied. The analog beamforming uses only one RF chain with PSs to transmit the signal which gives rise to the interference possibilities. The digital beamforming, on the other hand, uses individual RF chain for each antenna elements. This results into the extensive increase in the amount of energy consumption which overlooks the high throughput achieved by the digital beamformer. Thus the use of digital beamforming becomes unrealistic in practical communication scenario. The combination of analog and digital beamformer engenders a new concept i.e. the hybrid beamforming. In this thesis work, we have adopted

hybrid beamforming in the proposed mmWave-MIMO-NOMA network. The hybrid beamforming is capable of lowering the energy consumption by enabling the analog domain but with improved throughput. We have proposed a novel fuzzy-based hybrid beamforming which further lowers the energy consumption and qualify high SNIR compared to the existing hybrid beamformers. The performance nearly matches with that of the digital beamforming but with much higher energy efficiency. The proposed beamforming technique outperforms all other techniques in term of data rate also.

For a further enhancement of NOMA, this work provides a discussion on how interference in a network can be mitigated. Interference mitigation is a major concern in NOMA network since the same sub-carriers are serving multiple users. The intra-cell interference in NOMA network is avoided by implementing SIC at the receivers. But the ICI still exists in the multi-cellular network. In fact, it is the major source of interference in OMA networks also. Several frequency reuse techniques can be applied to mitigate the interference. Fractional frequency reuse can mitigate the interference efficiently at the cost of increased bandwidth efficiency. SFR provides improved bandwidth efficiency but the interference mitigation becomes lower than FFR. This work proposes a novel sectored fractional frequency reuse technique and demonstrates it in multi-cellular NOMA network. This proposed technique combines the benefits of both FFR and SFR i.e. it can mitigate the ICI efficiently while maintaining high bandwidth efficiency. The bandwidth splitting is further minimized in the proposed work which has facilitated the accumulation of large number of devices and user pairing of NOMA. This results in the improvement of SE than any other design.

Finally, the mmWave-MIMO-NOMA network is analysed in the real communication environment. Most previous works examine the performance of the network in ideal scenario. Specifically, this thesis schedules the users basing on their traffic class (real time and non-real time users) and data rate requirements. The real time users are prioritized over the non-real time users for sub-band allocation. Moreover, the users with higher data requirement (video data etc) are assigned with additional sub-band from the unused band than the users with low data required. The multi-level waterfilling algorithm is selected as the power allocation algorithm. Then the overall system performance is analysed via simulation which is proved to outperform the state-of-the art. This research is expected to benefit the researchers whose choice of interest lie in this very field of wireless communications.

## 7.2 Contribution of the Thesis

The work we have done in the thesis can be divided into three sectors. At first, a mmWave-MIMO-NOMA system model has been proposed and analyzed. In particular, a fuzzy based switching algorithm for sub-connected hybrid beamforming structure is presented. The key contributions of the system model are:

(i) To enable the phase shifters as per the requirement so as to reduce the energy consumption of the phase shifters.

(ii) To design the system so that it can achieve almost the similar data rate as the digital beamforming and the conventional fully connected hybrid structure but with a very lesser complex design and lower power consumption.

(iii) The switching algorithm helps to improve the signal to noise ratio of the mmWave links also.

(iv) The main aim is to enhance energy efficiency and improve system capacity through a less complex structure in contrast to the existing structures. The proposed model outperforms all other methods in terms of these parameters.

After that, since interference mitigation is a prime concern in 5G wireless networks, we propose a novel design of interference cancellation technique to mitigate the ICI in multi-cellular NOMA networks. The proposed sectored FFR is compared with other frequency reuse techniques. The key findings of the thesis are:

(i) The ICI caused by the neighboring cell is noticeably reduced than the conventional design. It is achieved by sectorizing each cell and assign sub-bands in a way so that they do not interfere with each other.

(ii) The proposed FFR issues the lowest allocation of sub-bands for a particular cell radius. Thus, we can save sub-bands in the proposed scheme. Also, the sumrate gets increased than the existing techniques for the proposed scheme.

(iii) The lower splitting of bandwidth makes it possible to accumulate huge devices per sector in a cell. Also, all the sub-bands are available in all the cells while the interference is lesser than the SFR configuration. Thus, it enhances the SE of the network extensively than all other frequency reuse scheme.

(iv) A low-complexity waterfilling-based power allocation technique is proposed which has been incorporated with a proportional fair scheduler and applied to the network. The performance of the network for proposed user scheduling algorithm is found to outperform other fairness schemes. It maximizes the sumrate of the system while maintaining high level of fairness.

(v) Finally, the whole scenario is considered in real communication environment. Resource allocation is achieved by taking into account the traffic class and data rate requirement of the users. this benefits the quality of service (QoS) of the users in real communication environment.

(vi) The overall capacity of the network is increased while maintaining very low ICI which outperform the state of the art.

Finally we incorporated the proposed FLC based beamforming algorithm in the proposed FFR based multi-cellular network. The system model is capable of combining all the benefits of the above mentioned techniques i.e. it increases the sum rate at moderate energy efficiency at minimum interference.

## 7.3 Future Work

Throughout this thesis, We considered the perfect channel state information in the work. So this work can act as a prior work to further examine the performance of the network for non-ideal conditions i.e. for imperfect channel state estimation. Furthermore, the physical layer security of the NOMA network presented in this work can be investigated by adopting a proper beam management design. The author intends to further enrich this work by incorporating the network in more practical scenario taking into account several users' criteria to enhance the QoS of the 5G network.

# LIST OF PUBLICATIONS

1. F. Tabassum, AKM N. Islam, M. S. Kaiser, "Performance Evaluation of Fuzzy Based Hybrid MIMO architecture for 5G-IoT Communication", International Conference on Data Science and Application (ICDSA 2019), December 2019, Jaipur, India.

2. F. Tabassum, AKM N. Islam, M. S. Kaiser, "Modified Fractional Frequency Reuse Scheme for Non-orthogonal Multiple Access Networks", 3rd International Conference on Smart Systems and Inventive Technology (ICSSIT 2020), August 2020, Tirunelveli, India.

# REFERENCES

[1] M. Zeng, A. Yadav, O. A. Dobre, G. I. Tsiropoulos, and H. V. Poor, "Capacity comparison between mimo-noma and mimo-oma with multiple users in a cluster," *IEEE Journal on Selected Areas in Communications*, vol. 35, no. 10, pp. 2413–2424, 2017.

[2] G. M. D. T. Forecast, "Cisco visual networking index: global mobile data traffic forecast update, 2017–2022," *Update*, vol. 2017, p. 2022, 2019.

[3] M. A. Almasi, H. Mehrpouyan, V. Vakilian, N. Behdad, and H. Jafarkhani, "A new reconfigurable antenna mimo architecture for mmwave communication," in *2018 IEEE International Conference on Communications (ICC)*. IEEE, 2018, pp. 1–7.

[4] K. C. Amy Nordrum and I. S. Staff, "Everything you need to know about 5g," 2017, accessed 22 august 2020. [Online]. Available: https://spectrum.ieee.org/video/telecom/wireless/everything-you-need-to-know-about-5g

[5] W. Shin, M. Vaezi, B. Lee, D. J. Love, J. Lee, and H. V. Poor, "Coordinated beamforming for multi-cell mimo-noma," *IEEE Communications Letters*, vol. 21, no. 1, pp. 84–87, 2016.

[6] S. M. R. Islam *et al.*, "Power-domain non-orthogonal multiple access (noma) in 5g systems: Potentials and challenges," *IEEE Commun. Surv. Tutor.*, vol. 19, no. 2, pp. 721–742, 2017.

[7] W. Shin, M. Vaezi, B. Lee, D. J. Love, J. Lee, and H. V. Poor, "Non-orthogonal multiple access in multi-cell networks: Theory, performance, and practical challenges," *IEEE Communications Magazine*, vol. 55, no. 10, pp. 176–183, 2017.

[8] Z. Ding, P. Fan, and H. V. Poor, "Impact of user pairing on 5g nonorthogonal multiple-access downlink transmissions," *IEEE Transactions on Vehicular Technology*, vol. 65, no. 8, pp. 6010–6023, 2016.

[9] K. Higuchi and A. Benjebbour, "Non-orthogonal multiple access (noma) with successive interference cancellation for future radio access," *IEICE Transactions on Communications*, vol. 98, no. 3, pp. 403–414, 2015.

[10] Y. Saito, A. Benjebbour, Y. Kishiyama, and T. Nakamura, "System-level performance evaluation of downlink non-orthogonal multiple access (noma)," in *2013 IEEE 24th Annual International Symposium on Personal, Indoor, and Mobile Radio Communications (PIMRC)*. IEEE, 2013, pp. 611–615.

[11] Y. Saito, Y. Kishiyama, A. Benjebbour, T. Nakamura, A. Li, and K. Higuchi, "Non-orthogonal multiple access (noma) for cellular future radio access," in *2013 IEEE 77th vehicular technology conference (VTC Spring)*. IEEE, 2013, pp. 1–5.

[12] Z. Yang, Z. Ding, P. Fan, and G. K. Karagiannidis, "On the performance of non-orthogonal multiple access systems with partial channel information," *IEEE Transactions on Communications*, vol. 64, no. 2, pp. 654–667, 2015.

[13] D. Wan, M. Wen, F. Ji, H. Yu, and F. Chen, "Non-orthogonal multiple access for cooperative communications: Challenges, opportunities, and trends," *IEEE Wireless Communications*, vol. 25, no. 2, pp. 109–117, 2018.

[14] Z. Ding, Z. Yang, P. Fan, and H. V. Poor, "On the performance of non-orthogonal multiple access in 5g systems with randomly deployed users," *IEEE signal processing letters*, vol. 21, no. 12, pp. 1501–1505, 2014.

[15] S. K. Sharma, M. Patwary, and S. Chatzinotas, "Multiple access techniques for next generation wireless: Recent advances and future perspectives," *EAI Endorsed Transactions on Wireless Spectrum*, vol. 2, no. 7, 2016.

[16] S. R. Islam, M. Zeng, O. A. Dobre, and K.-S. Kwak, "Nonorthogonal multiple access (noma): How it meets 5g and beyond," *Wiley 5G Ref: The Essential 5G Reference Online*, pp. 1–28, 2019.

[17] Y. Zhou, H. Luo, R. Li, and J. Wang, "A dynamic states reduction message passing algorithm for sparse code multiple access," in *2016 Wireless Telecommunications Symposium (WTS)*. IEEE, 2016, pp. 1–5.

[18] X. Dai, S. Chen, S. Sun, S. Kang, Y. Wang, Z. Shen, and J. Xu, "Successive interference cancelation amenable multiple access (sama) for future wireless communications," in *2014 IEEE International Conference on Communication Systems*. IEEE, 2014, pp. 222–226.

[19] S. Zhang, B. Xiao, K. Xiao, Z. Chen, and B. Xia, "Design and analysis of irregular sparse code multiple access," in *2015 International Conference on Wireless Communications & Signal Processing (WCSP)*. IEEE, 2015, pp. 1–5.

[20] B. Xiao, K. Xiao, S. Zhang, Z. Chen, B. Xia, and H. Liu, "Iterative detection and decoding for scma systems with ldpc codes," in *2015 International Conference on Wireless Communications & Signal Processing (WCSP)*. IEEE, 2015, pp. 1–5.

[21] S. R. Islam, M. Zeng, O. A. Dobre, and K.-S. Kwak, "Resource allocation for downlink noma systems: Key techniques and open issues," *IEEE Wireless Communications*, vol. 25, no. 2, pp. 40–47, 2018.

[22] N. Otao, Y. Kishiyama, and K. Higuchi, "Performance of non-orthogonal access with sic in cellular downlink using proportional fair-based resource allocation," in *2012 ISWCS*. IEEE, 2012, pp. 476–480.

[23] J. Cui, Y. Liu, Z. Ding, P. Fan, and A. Nallanathan, "Optimal user scheduling and power allocation for millimeter wave noma systems," *IEEE Transactions on Wireless Communications*, vol. 17, no. 3, pp. 1502–1517, 2017.

[24] L. Dai, B. Wang, M. Peng, and S. Chen, "Hybrid precoding-based millimeter-wave massive mimo-noma with simultaneous wireless information and power transfer," *IEEE Journal on Selected Areas in Communications*, vol. 37, no. 1, pp. 131–141, 2018.

[25] Z. Xiao, L. Zhu, J. Choi, P. Xia, and X.-G. Xia, "Joint power allocation and beamforming for non-orthogonal multiple access (noma) in 5g millimeter wave communications," *IEEE Transactions on Wireless Communications*, vol. 17, no. 5, pp. 2961–2974, 2018.

[26] L. Zhu, J. Zhang, Z. Xiao, X. Cao, D. O. Wu, and X.-G. Xia, "Joint power control and beamforming for uplink non-orthogonal multiple access in 5g millimeter-wave communications," *IEEE Transactions on Wireless Communications*, vol. 17, no. 9, pp. 6177–6189, 2018.

[27] S. A. R. Naqvi and S. A. Hassan, "Combining noma and mmwave technology for cellular communication," in *2016 IEEE 84th Vehicular Technology Conference (VTC-Fall)*. IEEE, 2016, pp. 1–5.

[28] Z. Wei, L. Zhao, J. Guo, D. W. K. Ng, and J. Yuan, "A multi-beam noma framework for hybrid mmwave systems," in *2018 IEEE International Conference on Communications (ICC)*. IEEE, 2018, pp. 1–7.

[29] Z. Xiao, P. Xia, and X.-G. Xia, "Full-duplex millimeter-wave communication," *IEEE Wireless Communications*, vol. 24, no. 6, pp. 136–143, 2017.

[30] M. Xiao, *et al.*, "Millimeter wave communications for future mobile networks," *IEEE Journal on Selected Areas in Communications*, vol. 35, no. 9, pp. 1909–1935, 2017.

[31] J. G. Andrews, T. Bai, M. N. Kulkarni, A. Alkhateeb, A. K. Gupta, and R. W. Heath, "Modeling and analyzing millimeter wave cellular systems," *IEEE Transactions on Communications*, vol. 65, no. 1, pp. 403–430, 2016.

[32] Y. Zhou, V. W. Wong, and R. Schober, "Coverage and rate analysis of millimeter wave noma networks with beam misalignment," *IEEE Transactions on Wireless Communications*, vol. 17, no. 12, pp. 8211–8227, 2018.

[33] M. A. Almasi, H. Mehrpouyan, D. Matolak, C. Pan, and M. Elkashlan, "Reconfigurable antenna multiple access for 5g mmwave systems," in *2018 IEEE International Conference on Communications Workshops (ICC Workshops)*. IEEE, 2018, pp. 1–6.

[34] M. A. Almasi, H. Mehrpouyan, V. Vakilian, N. Behdad, and H. Jafarkhani, "Reconfigurable antennas in mmwave mimo systems," *arXiv preprint arXiv:1710.05111*, 2017.

[35] Z. Ding, P. Fan, and H. V. Poor, "Random beamforming in millimeter-wave noma networks," *IEEE access*, vol. 5, pp. 7667–7681, 2017.

[36] Z. Xiao, T. He, P. Xia, and X.-G. Xia, "Hierarchical codebook design for beamforming training in millimeter-wave communication," *IEEE Transactions on Wireless Communications*, vol. 15, no. 5, pp. 3380–3392, 2016.

[37] H. Xie, F. Gao, S. Zhang, and S. Jin, "A unified transmission strategy for tdd/fdd massive mimo systems with spatial basis expansion model," *IEEE Transactions on Vehicular Technology*, vol. 66, no. 4, pp. 3170–3184, 2016.

[38] P. V. Amadori and C. Masouros, "Low rf-complexity millimeter-wave beamspace-mimo systems by beam selection," *IEEE Transactions on Communications*, vol. 63, no. 6, pp. 2212–2223, 2015.

[39] B. Wang, L. Dai, Z. Wang, N. Ge, and S. Zhou, "Spectrum and energy-efficient beamspace mimo-noma for millimeter-wave communications using lens antenna array," *IEEE Journal on Selected Areas in Communications*, vol. 35, no. 10, pp. 2370–2382, 2017.

[40] X. Gao, L. Dai, S. Han, I. Chih-Lin, and R. W. Heath, "Energy-efficient hybrid analog and digital precoding for mmwave mimo systems with large antenna arrays," *IEEE Journal on Selected Areas in Communications*, vol. 34, no. 4, pp. 998–1009, 2016.

[41] A. Alkhateeb, G. Leus, and R. W. Heath, "Limited feedback hybrid precoding for multi-user millimeter wave systems," *IEEE transactions on wireless communications*, vol. 14, no. 11, pp. 6481–6494, 2015.

[42] A. Alkhateeb, R. W. Heath, and G. Leus, "Achievable rates of multi-user millimeter wave systems with hybrid precoding," in *2015 IEEE International Conference on Communication Workshop (ICCW)*. IEEE, 2015, pp. 1232–1237.

[43] W. Wu and D. Liu, "Non-orthogonal multiple access based hybrid beamforming in 5g mmwave systems," in *2017 IEEE 28th Annual International Symposium on Personal, Indoor, and Mobile Radio Communications (PIMRC)*. IEEE, 2017, pp. 1–7.

[44] L. Zhu, J. Zhang, Z. Xiao, X. Cao, D. O. Wu, and X.-G. Xia, "Millimeter-wave noma with user grouping, power allocation and hybrid beamforming," *IEEE Transactions on Wireless Communications*, vol. 18, no. 11, pp. 5065–5079, 2019.

[45] X. Chen, Z. Zhang, C. Zhong, D. W. K. Ng, and R. Jia, "Exploiting inter-user interference for secure massive non-orthogonal multiple access," *IEEE Journal on Selected Areas in Communications*, vol. 36, no. 4, pp. 788–801, 2018.

[46] Y. Sun, D. W. K. Ng, J. Zhu, and R. Schober, "Robust and secure resource allocation for full-duplex miso multicarrier noma systems," *IEEE Transactions on Communications*, vol. 66, no. 9, pp. 4119–4137, 2018.

[47] Y. Cao, N. Zhao, Y. Chen, M. Jin, Z. Ding, Y. Li, and F. R. Yu, "Secure transmission via beamforming optimization for noma networks," *IEEE Wireless Communications*, vol. 27, no. 1, pp. 193–199, 2019.

[48] M. S. Kaiser, K. T. Lwin, M. Mahmud, D. Hajializadeh, T. Chaipimonplin, A. Sarhan, and M. A. Hossain, "Advances in crowd analysis for urban applications

through urban event detection," *IEEE Transactions on Intelligent Transportation Systems*, vol. 19, no. 10, pp. 3092–3112, 2018.

[49] J. Kim, T. Kim, J. Noh, and S. Cho, "Fractional frequency reuse scheme for device to device communication underlaying cellular on wireless multimedia sensor networks," *Sensors*, vol. 18, no. 8, p. 2661, 2018.

[50] L. Huo and D. Jiang, "Stackelberg game-based energy-efficient resource allocation for 5g cellular networks," *Telecommunication Systems*, vol. 72, no. 3, pp. 377–388, 2019.

[51] T. D. Novlan, R. K. Ganti, A. Ghosh, and J. G. Andrews, "Analytical evaluation of fractional frequency reuse for ofdma cellular networks," *IEEE Transactions on wireless communications*, vol. 10, no. 12, pp. 4294–4305, 2011.

[52] Z. F. Smriti, M. S. Kaiser, and K. M. Ahmed, "Interference mitigation for ofdm-based joint macro-femto cellular networks," *Netw. and Communic. Technol.*, vol. 1, no. 1, pp. 103–110, 2012.

[53] J. García-Morales, G. Femenias, and F. Riera-Palou, "Statistical analysis and optimization of ffr/sfr-aided ofdma-based multi-cellular networks," in *2016 IEEE SSP*, 2016, pp. 1–5.

[54] Z. Xu, G. Y. Li, C. Yang, and X. Zhu, "Throughput and optimal threshold for ffr schemes in ofdma cellular networks," *IEEE Trans. Wirel. Commun.*, vol. 11, no. 8, pp. 2776–2785, 2012.

[55] S. U. Abdullahi, J. Liu, and S. A. Mohadeskasaei, "Stochastic geometry based framework for coverage and rate in heterogeneous networks with sectored fractional frequency reuse," *Am. J. Netw. Commun.*, vol. 6, no. 1, pp. 20–34, 2017.

[56] K. Mehmood, M. T. Niaz, and H. S. Kim, "Dynamic fractional frequency reuse diversity design for intercell interference mitigation in nonorthogonal multiple access multicellular networks," *Wirel. Commun. Mob. Comput.*, vol. 2018, 2018.

[57] R. Ghaffar and R. Knopp, "Fractional frequency reuse and interference suppression for ofdma networks," in *8th International Symposium on Modeling and Optimization in Mobile, Ad Hoc, and Wireless Networks*. IEEE, 2010, pp. 273–277.

[58] Y. Umeda and K. Higuchi, "Efficient adaptive frequency partitioning in ofdma downlink with fractional frequency reuse," in *2011 International Symposium on Intelligent Signal Processing and Communications Systems (ISPACS)*. IEEE, 2011, pp. 1–5.

[59] Y. Lan, A. Benjebbour, A. Li, and A. Harada, "Efficient and dynamic fractional frequency reuse for downlink non-orthogonal multiple access," in *2014 IEEE 79th Vehicular Technology Conference (VTC Spring)*. IEEE, 2014, pp. 1–5.

[60] J. A. del Peral-Rosado, R. Raulefs, J. A. López-Salcedo, and G. Seco-Granados, "Survey of cellular mobile radio localization methods: From 1g to 5g," *IEEE Communications Surveys & Tutorials*, vol. 20, no. 2, pp. 1124–1148, 2017.

[61] H. Viswanathan and M. Weldon, "The past, present, and future of mobile communications," *Bell Labs Technical Journal*, vol. 19, pp. 8–21, 2014.

[62] M. S. Afaqui, E. Garcia-Villegas, and E. Lopez-Aguilera, "Ieee 802.11 ax: Challenges and requirements for future high efficiency wifi," *IEEE Wireless Communications*, vol. 24, no. 3, pp. 130–137, 2016.

[63] Y. Zhang, H. Cao, M. Zhou, and L. Yang, "Spectral efficiency maximization for uplink cell-free massive mimo-noma networks," in *2019 IEEE ICC Workshops*, 2019, pp. 1–6.

[64] Z. Wei, "Performance analysis and design of non-orthogonal multiple access for wireless communications," *arXiv preprint arXiv:1910.00946*, 2019.

[65] L. Dai, B. Wang, Z. Ding, Z. Wang, S. Chen, and L. Hanzo, "A survey of non-orthogonal multiple access for 5g," *IEEE communications surveys & tutorials*, vol. 20, no. 3, pp. 2294–2323, 2018.

[66] I. Bukar, "Spectrally efficient non-orthogonal multiple access (noma) techniques for future generation mobile systems," Ph.D. dissertation, University of Sussex, 2017.

[67] M. Z. Chowdhury, M. T. Hossan, and Y. M. Jang, "Interference management based on rt/nrt traffic classification for ffr-aided small cell/macrocell heterogeneous networks," *IEEE Access*, vol. 6, pp. 31 340–31 358, 2018.

[68] T. Lv, Y. Ma, J. Zeng, and P. T. Mathiopoulos, "Millimeter-wave noma transmission in cellular m2m communications for internet of things," *IEEE Internet of Things Journal*, vol. 5, no. 3, pp. 1989–2000, 2018.

[69] M. A. Almasi, M. Vaezi, and H. Mehrpouyan, "Impact of beam misalignment on hybrid beamforming noma for mmwave communications," *IEEE Transactions on Communications*, vol. 67, no. 6, pp. 4505–4518, 2019.

[70] R. Mendez-Rial, C. Rusu, N. González-Prelcic, A. Alkhateeb, and R. W. Heath, "Hybrid mimo architectures for millimeter wave communications: Phase shifters or switches?" *Ieee Access*, vol. 4, pp. 247–267, 2016.

[71] E. Vlachos, A. Kaushik, and J. Thompson, "Energy efficient transmitter with low resolution dacs for massive mimo with partially connected hybrid architecture," in *2018 IEEE 87th Vehicular Technology Conference (VTC Spring)*. IEEE, 2018, pp. 1–5.

[72] T. E. Bogale, L. Le, A. Haghighat, and L. Vandendorpe, "On the number of rf chains and phase shifters, and scheduling design with hybrid analog-digital beamforming," *IEEE Tran Wireless (To appear)*, vol. 15, 08 2015.

[73] B. Wang, L. Dai, X. Gao, and L. Hanzo, "Beamspace mimo-noma for millimeter-wave communications using lens antenna arrays," in *2017 IEEE 86th Vehicular Technology Conference (VTC-Fall)*. IEEE, 2017, pp. 1–5.

[74] A. Salh, L. Audah, N. S. M. Shah, and S. A. Hamzah, "Trade-off energy and spectral efficiency in a downlink massive mimo system," *Wireless Personal Communications*, vol. 106, no. 2, pp. 897–910, 2019.

[75] I. Ahmed, H. Khammari, A. Shahid, A. Musa, K. S. Kim, E. De Poorter, and I. Moerman, "A survey on hybrid beamforming techniques in 5g: Architecture and system model perspectives," *IEEE Communications Surveys & Tutorials*, vol. 20, no. 4, pp. 3060–3097, 2018.

[76] X. Yu, J.-C. Shen, J. Zhang, and K. B. Letaief, "Alternating minimization algorithms for hybrid precoding in millimeter wave mimo systems," *IEEE Journal of Selected Topics in Signal Processing*, vol. 10, no. 3, pp. 485–500, 2016.

[77] C. Xu, R. Ye, Y. Huang, S. He, and C. Zhang, "Hybrid precoding for broadband millimeter-wave communication systems with partial csi," *IEEE Access*, vol. 6, pp. 50 891–50 900, 2018.

[78] A. F. Molisch, V. V. Ratnam, S. Han, Z. Li, S. L. H. Nguyen, L. Li, and K. Haneda, "Hybrid beamforming for massive mimo: A survey," *IEEE Communications Magazine*, vol. 55, no. 9, pp. 134–141, 2017.

[79] P. Zhao and Z. Wang, "Hybrid precoding for millimeter wave communications with fully connected subarrays," *IEEE Communications Letters*, vol. 22, no. 10, pp. 2160–2163, 2018.

[80] I. Chafaa and M. Djeddou, "Improved channel estimation in mmwave communication system," in *2017 Seminar on Detection Systems Architectures and Technologies (DAT)*. IEEE, 2017, pp. 1–5.

[81] Y. Peng, Y. Li, and P. Wang, "An enhanced channel estimation method for millimeter wave systems with massive antenna arrays," *IEEE Communications Letters*, vol. 19, no. 9, pp. 1592–1595, 2015.

[82] M. F. Uddin, "Energy efficiency maximization by joint transmission scheduling and resource allocation in downlink noma cellular networks," *Computer Networks*, vol. 159, pp. 37–50, 2019.

[83] C. Zheng and Z. Hailin, "A quasi-perfect resource allocation scheme for optimizing the performance of cell-edge users in ffr-aided lte-a multicell networks," *IEEE Commun. Lett.*, vol. 23, no. 5, pp. 918–921, 2019.

[84] R. Y. Chang, Z. Tao, J. Zhang, and C. . Kuo, "A graph approach to dynamic fractional frequency reuse (ffr) in multi-cell ofdma networks," in *2009 IEEE International Conference on Communications*, 2009, pp. 1–6.

[85] S. U. Abdullahi *et al.*, "Efficient resource allocation with improved interference mitigation in ffr-aided ofdma heterogeneous networks," *J Elec Sci Tech*, vol. 17, no. 1, pp. 73–89, 2019.

[86] S. Hashima *et al.*, "Analysis and comparison of fractional frequency reuse schemes based on worst case signal to interference power ratio in ofdma uplink," 04 2014.

[87] S. Tao, H. Yu, Q. Li, X. Bai, and Y. Tang, "Power allocation of non-orthogonal multiple access based on dynamic user priority for indoor qos-guaranteed visible light communication networks," *Applied Sciences*, vol. 8, no. 8, p. 1219, 2018.